Accepted Manuscript

Design, synthesis and biological screening of 2-aminobenzamides as selective HDAC3 inhibitors with promising anticancer effects

Prakruti Trivedi, Nilanjan Adhikari, Sk. Abdul Amin, Tarun Jha, Balaram Ghosh

PII: S0928-0987(18)30398-1
DOI: doi:10.1016/j.ejps.2018.08.030
Reference: PHASCI 4667

To appear in: *European Journal of Pharmaceutical Sciences*

Received date: 5 June 2018
Revised date: 11 August 2018
Accepted date: 23 August 2018

Please cite this article as: Prakruti Trivedi, Nilanjan Adhikari, Sk. Abdul Amin, Tarun Jha, Balaram Ghosh , Design, synthesis and biological screening of 2-aminobenzamides as selective HDAC3 inhibitors with promising anticancer effects. Phasci (2018), doi:10.1016/j.ejps.2018.08.030

Design, synthesis and biological screening of 2-aminobenzamides as selective HDAC3 inhibitors with promising anticancer effects

Prakruti Trivedi[a], Nilanjan Adhikari[b,#], Sk. Abdul Amin[b], Tarun Jha[b,*], Balaram Ghosh[a*]
[a]*Department of Pharmacy, BITS-Pilani, Hyderabad Campus, Shameerpet, Hyderabad, India, 500078*
[b]*Natural Science Laboratory, Division of Medicinal and Pharmaceutical Chemistry, Department of Pharmaceutical Technology, Jadavpur University, Kolkata, India 700032*

[#]Present Address:

School of Pharmaceutical Technology, ADAMAS University, Barasat-Barrackpore Road, P. O. Jagannathpur, Kolkata – 700126, West Bengal, India

*****corresponding author: (T. Jha) tjupharm@yahoo.com; (B. Ghosh) balaram@hyderabad.bitspilani.ac.in

***Corresponding author**
Balaram Ghosh, PhD
Room. A016, Department of Pharmacy
Birla Institute of Technology & Sciences-Pilani,
Hyderabad Campus, Jawahar Nagar, Shameerpet,
Hyderabad- 500 078, India
E-mail: balaram@hyderabad.bits-pilani.ac.in
Phone# 91-406-630-3639 (Office)
91-986-694-1923 (Cell)
Fax# 91-406-630-3998

Abstract

Histone deacetylases (HDACs) have been found as a potential target for anticancer therapy. A number of HDAC inhibitors have been used pre-clinically and clinically as anticancer agents. In the current study, we have designed and synthesized compound **12a** by combining the scaffolds of **CI-994** and **BG45.** Moreover, the structure of compound **12a** was optimized and a series of 2-aminobenzamide derivatives were synthesized further. These compounds were tested for their HDAC inhibitory activity and found to be efficient HDAC inhibitors. Compound **26c** showed

11.68-fold HDAC3 selectivity over pan HDACs, better than the prototype HDAC3 inhibitor **BG-45**. Most of these compounds exhibited antiproliferative activity in both B16F10 and HeLa cell lines. Particularly, compound **26c** exhibited better antitumor efficacy in the cell lines compared to the prototype inhibitors **CI-994** and **BG45.** It was also found to promote apoptosis as well as induced significant cell growth arrest in the G2/M phase of cell cycle in B16F10 melanoma cells. This work may provide significant insight regarding structural information to design newer small molecule HDAC3 inhibitors to fight against the target specific malignancies in future.

Keywords: Anticancer agent; HDAC inhibitor; isoform-selective HDAC3 inhibitor; density functional theory (DFT); 2-aminobenzamide; structure-activity relationship (SAR)

List of abbreviations

B16F10	murine melanoma cells
$CDCl_3$	deuterated chloroform
CTCL	cutaneous T-cell lymphoma
DCM	dichloromethane
DFT	density functional theory
DMAP	4-Dimethylaminopyridine
DMEM	Dulbecco's modified Eagle's media
DMF	dimethylformamide
DMSO	dimethyl sulphoxide
DMSO-d6	deuterated dimethyl sulphoxide
EDC	1-Ethyl-3-(3-dimethylaminopropyl)carbodiimide
ESI	electron spray ionization

EtOAc	ethyl acetate
FITC	fluorescein isothiocyanate
HCl	hydrochloric acid
HeLa	human cervical cancer cell line
HOMO	highest energy occupied molecular orbital
HPLC	high performance liquid chromatography
IC_{50}	half maximal inhibitory concentration
LC-MS	liquid chromatography–mass spectrometry
LUMO	lowest energy unoccupied molecular orbital
MTT	3-(4,5-dimethylthiazol-2-yl)-2,5-di-phenyltetrazolium bromide
Na_2SO_4	sodium sulphate
$NaHCO_3$	sodium bicarbonate
NCOR1	Nuclear receptor corepressor 1
NMR	nuclear magnetic resonance
PBS	phosphate buffered saline
PI	propidium iodide
ppm	parts per million
PTCL	peripheral T-cell lymphoma
Rt	retention time
RT	room temperature
SAHA	suberoylanilide hydroxamic acid
THF	tetrahydrofuran
TLC	thin layer chromatography

USFDA	US food and drug administrations
ZBG	zinc binding group

1. Introduction

Cancer is one of the major causes of death worldwide. Even though progress has been made in prevention and treatment of cancer, still cancer burden is increasing globally (1). In past few years, deacetylation of histone has been considered as a promising target for anticancer therapy. Histone deacetylases (HDACs) are a family of enzymes which deacetylate the lysine residue of core histone and other cellular proteins and subsequently results in chromatin condensation and transcriptional repression (2-4). These epigenetic alterations by HDACs are involved in suppressing the gene transcription and finally lead to the silencing of tumor suppressor genes. Abnormal expression of various HDACs has been reported in numerous cancer cell lines and tumor tissues (5). HDAC inhibitors promote tumor cell death by inducing apoptosis, cell cycle arrest, senescence, differentiation, autophagy, etc. Therefore, HDAC inhibition has emerged out as a potential anticancer target (6-9).

Till date, a total of 18 HDACs have been identified and these HDACs are grouped into four distinct classes depending on their cellular localization, size and the number of active sites along with structural homology to yeast (10). Class I HDACs consists of four members namely HDAC 1, 2, 3 and 8 whereas class IV contains only one HDAC namely HDAC11. However, class II is subdivided into two groups, i.e., class IIa and class IIb. HDACs 4, 5, 7 and 9 belong to class IIa subfamily whereas HDAC6 and 10 belong to class IIb subfamily. Class III HDACs are basically sirtuins (sirtuins 1-7) which are completely different from the other class HDACs. These class I, II and IV HDACs are zinc-dependent while sirtuins are NAD^+ dependent metalloenzymes (11, 12).

Since past few years, a number of HDAC inhibitors have been studied pre-clinically and clinically for various cancers (**Figure 1**).

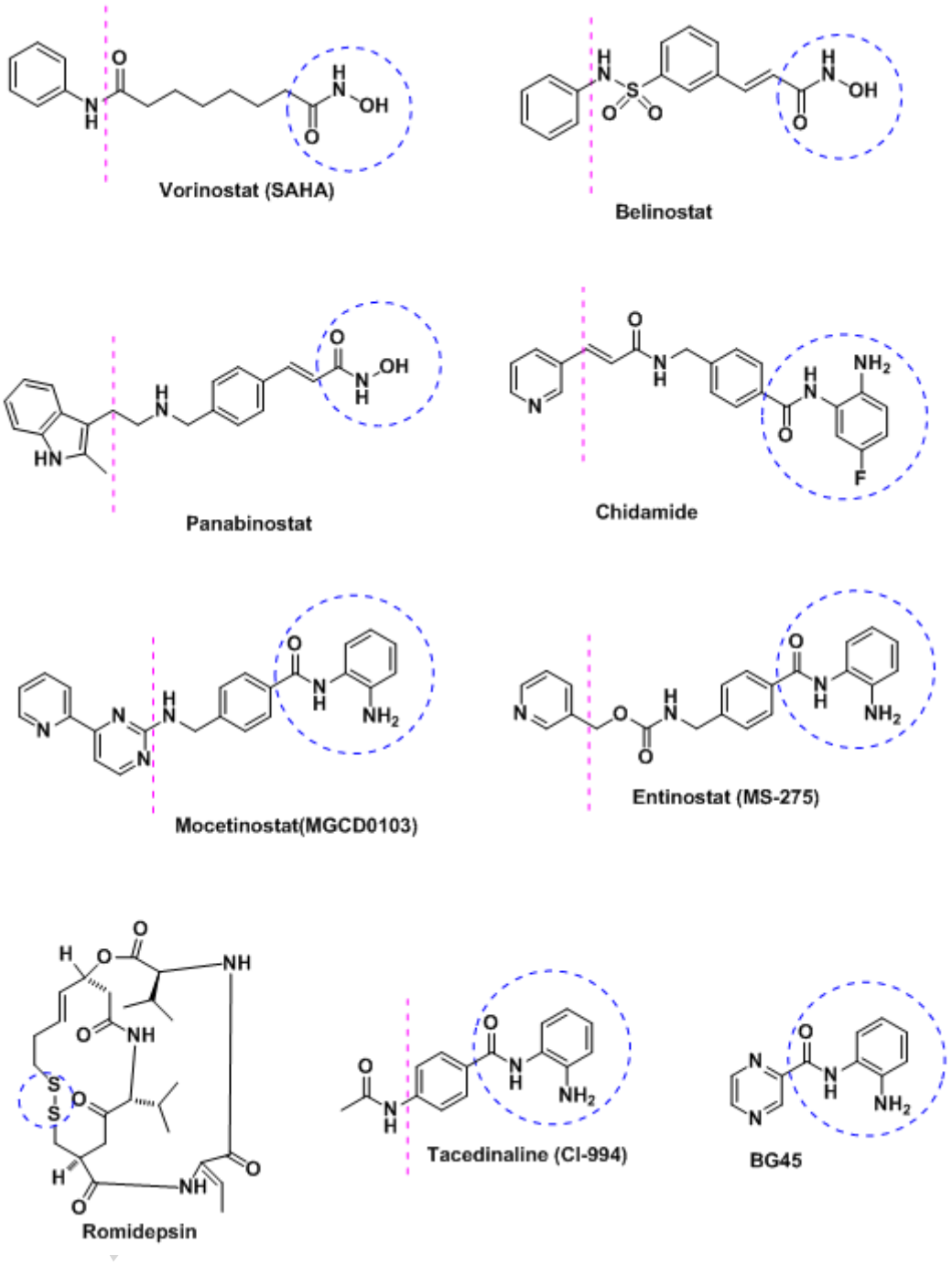

Figure 1. Potential HDAC inhibitors [clinically approved and in clinical trials]

Four of them have been approved by USFDA for clinical use. Vorinostat (SAHA) has been approved for the treatment of cutaneous T-cell lymphoma (CTCL), whereas romidepsin is

approved for both cutaneous T-cell lymphoma (CTCL) as well as peripheral T-cell lymphoma (PTCL). Again, belinostat is utilized for peripheral T-cell lymphoma and panobinostat is approved for multiple myeloma. Chidamide has been approved for peripheral T-cell lymphoma in China (13). Many other promising HDAC inhibitors such as entinostat (MS-275), mocetinostat (MGCD-0103), tacedinaline (CI-994) are now in clinical trials for the treatment of different types of cancers (14-18). Generally, HDAC inhibitors have a common pharmacophore model (**Figure 2**) which includes three regions, i.e., one cap group or surface recognition domain, a linker function and a zinc binding group (ZBG) (19).

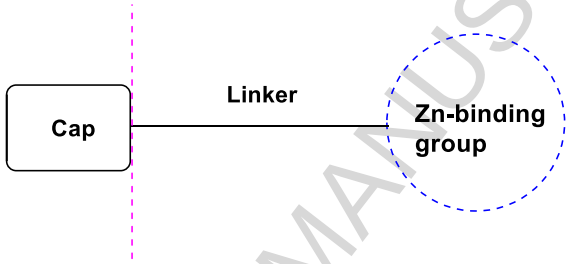

Figure 2. General pharmacophore model for HDAC inhibitors

The first generation HDAC inhibitors (such as vorinostat, romidepsin, belinostat and panobinostat) containing hydroxamate function as ZBG having pan HDAC inhibitory effects are found to be effective anticancer agents (**Figure 1**).

Among different HDACs, histone deacetylase 3 (HDAC3) has been found to play pivotal roles in the cancer cell proliferation, migration and apoptosis (20) along with DNA repair, genome stabilization and maintaining structural integrity of chromatin as well as histone deacetylation mechanisms during cell cycle progression and apoptosis (21-23). Overexpression of HDAC3 has been attributed in numerous cancers such as breast cancer (24, 25), lung cancer (26), liver cancer (27), colon cancer (28), leukemia (29), multiple myeloma (30), lymphoma (31), melanoma (32)

and glioma (33). Therefore, inhibitors targeted to HDAC3 may be considered as a useful tool to combat various malignancies.

In recent scenario to achieve increased selectivity and specificity, other ZBGs (such as benzamides, thiols, sulphamides) have been taken into consideration (34). In general, benzamides are found to inhibit class I HDACs (namely entinostat, mocetinostat and **CI-994**) (35, 36). Modifications of the cap region having supremacy to target selective HDAC as it not only binds to the enzyme surface but also forms complexes present nearby. These could help to design the selective HDAC inhibitors (37, 38). Compounds possessing 2-aminobenzamide moiety as zinc binding group (ZBG) has already been proven to execute selectivity towards HDAC3 with promising anticancer properties (39-41). Depending on some crucial observations obtained by our recent molecular modeling study (42) on selective HDAC3 inhibitors, newer HDAC3 inhibitors are designed in the present work. These observations for designing newer HDAC3 inhibitors are furnished below:

1. The free amino group of benzamide moiety may serve as hydrogen bonding interaction. Therefore, no substitution was made here.
2. Hydrophobicity of the phenyl group is crucial for HDAC3 inhibition. Not only that, no bulky steric and hydrophobic substitution at 5^{th} position of the phenyl group of benzamide moiety was considered for designing HDAC3 inhibitor as it was unfavorable for HDAC3 inhibition.
3. Smaller electron-withdrawing substituents (such as fluoro) at the *para* position of the benzamide moiety was considered for designing newer HDAC3 inhibitors as it may favor HDAC3 selectivity.

4. Carboxamide function attached to the benzamide scaffold was kept intact as the carbonyl group is necessary for hydrogen bonding and amide group coordinated to the catalytic Zn^{2+} ion.
5. Steric and hydrophobic aryl linker function was taken into consideration.
6. Smaller aryl cap group was taken into account.

BG45, a benzamide-based class I HDAC inhibitor with preferential selectivity towards HDAC3 showed a significant inhibition of cellular proliferation in multiple myeloma *in vitro*. Moreover, it was also found to be effective *in vivo* in arresting tumor growth as evidenced in the murine xenograft model of multiple myeloma (43). In the present study, we have designed and synthesized a series of novel benzamides by modifying the cap region of **BG45** in order to increase selectivity and efficacy towards HDAC3. These novel compounds were screened for their potency and selectivity for HDAC3 enzyme in the *in vitro* enzyme inhibition assay and for their anti-proliferative efficiency on different cancer cell lines.

2. Results and Discussion

2.1. Designing of benzamide-based HDAC3 inhibitors

Taking into account the density functional theory (DFT)-energy minimized electrostatic potential maps of **BG45** and **CI-994** (both are prototype isoform-selective HDAC inhibitors), it is observed that there is only a slight difference between them (**Figure 3**).

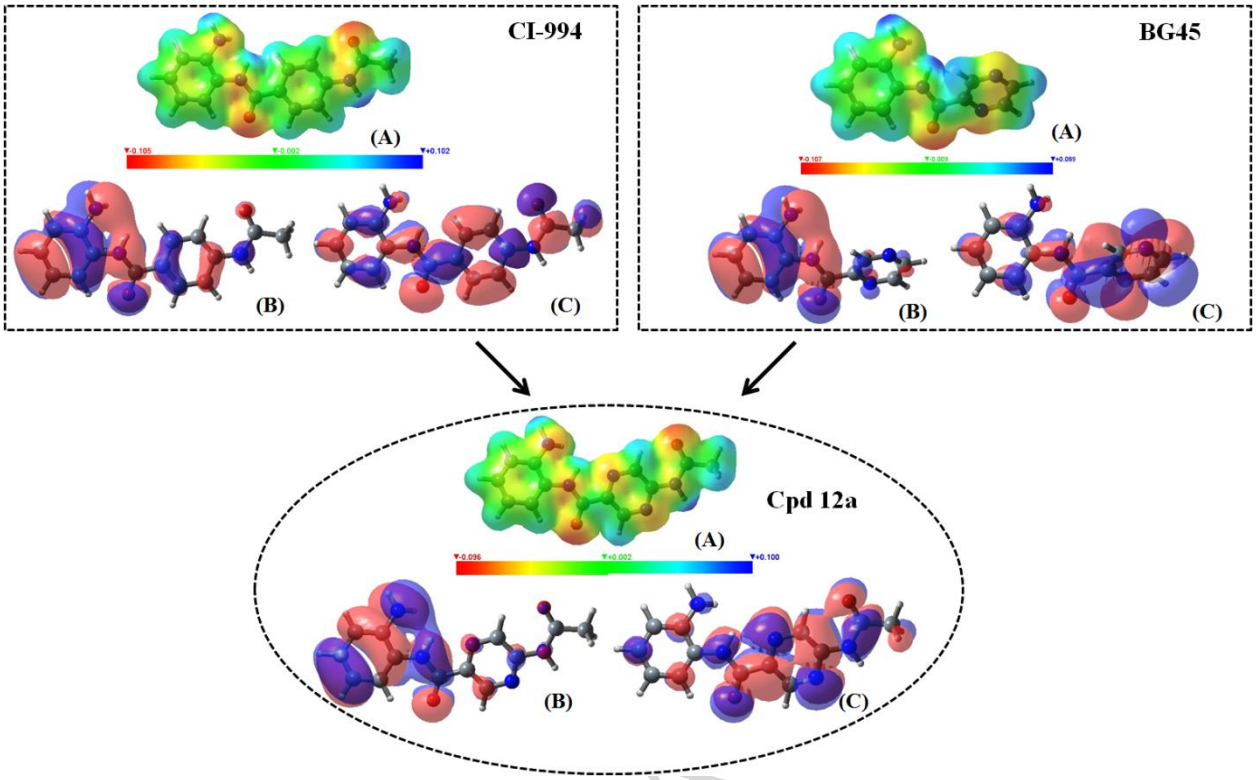

Figure 3. Designing of the initial hit molecule compound **12a** combining the structures of **CI-994** and **BG45** [(A): Electrostatic potential map; (B): HOMO orbital electron density map; (C): LUMO orbital electron density map].

Comparing activities of **CI-994** and **BG45**, it is observed that both of these molecules exhibit similar efficacy in HDAC3 inhibition. However, **BG45** is smaller in size or shorter in length compared to **CI-994**. Therefore, it may be inferred that as both of these molecules comprise the carboxybenzamide moiety, the pyrazine scaffold obviously possesses a positive influence on HDAC isoform selectivity. Comparing their electrostatic potential maps, it may be assumed that due to the higher electron-rich region (yellow) imparted by both of the nitrogen atoms of the pyrazine ring (**Figure 3**), **BG45** produces more HDAC3 inhibition compared to **CI-994**. Therefore, the phenyl ring of **CI-994** has been replaced with that pyrazine scaffold in compound

12a to judge whether the activity will increase or not. Interestingly, it displays both the features of **BG45** and **CI-994** (**Figure 4**).

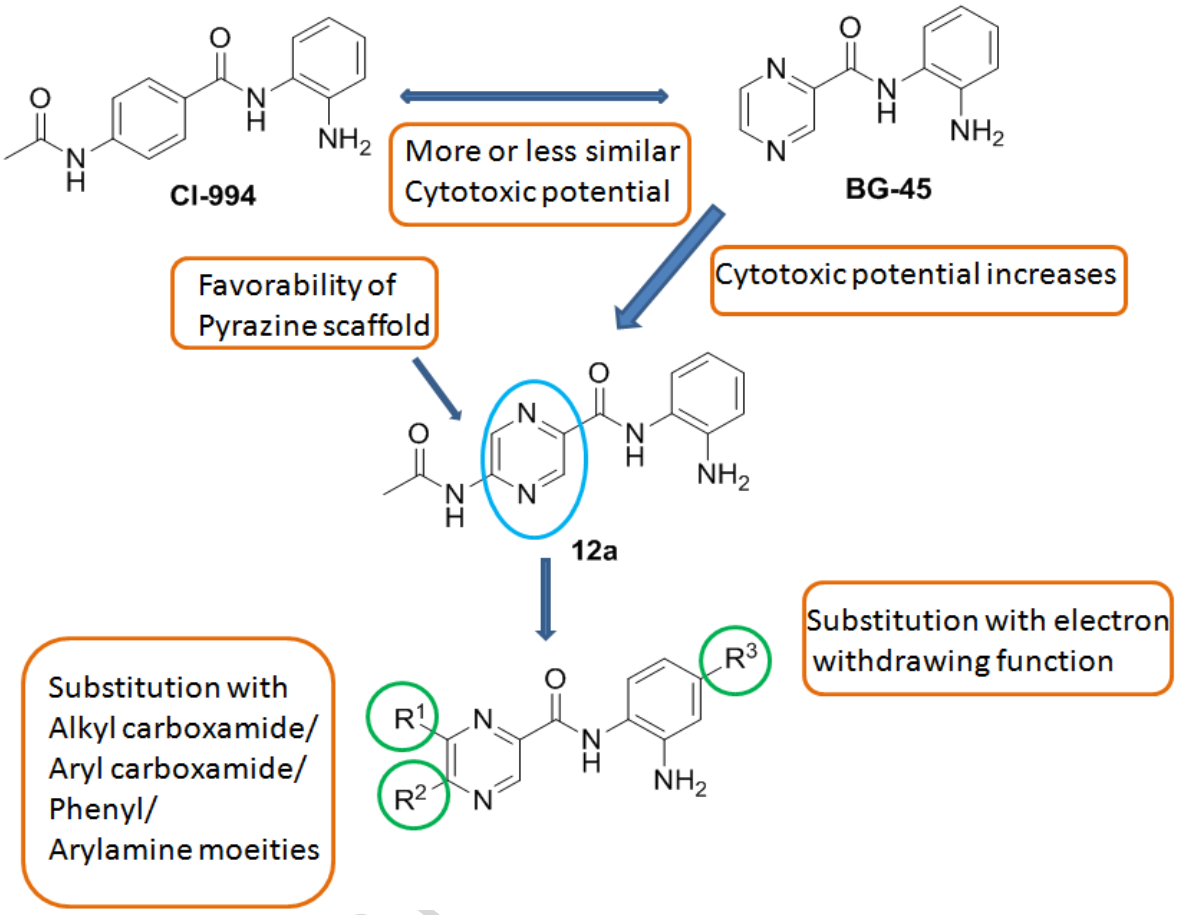

Figure 4. Designing of **BG45**-derived compounds

Nevertheless, the electrostatic potential map reveals that compound **12a** consists of more electronegative regions (yellow) compared to both **BG45** and **CI-994** (**Figure 3**). Moreover, the HOMO-LUMO electron density maps of both **BG45** and compound **12a** suggest that both of the HOMO and LUMO orbitals are located terminally and the LUMO orbitals of both these compounds comprise the overlapping feature of both the nucleophilic (blue) and electrophilic (red) regions at the pyrazine ring system (**Figure 3**). It clearly implies the ability of the pyrazine ring to involve charge transfer mechanisms or π-π interaction. Interestingly, it has been found

that compound **12a** results in better efficacy regarding both HDAC3 inhibition as well as cellular toxicity which strongly implicated the importance of pyrazine scaffold in the molecular structure for exerting better efficacy.

Considering compound **12a** as an initial hit molecule, newer molecules have been designed and synthesized by substitution at the *para* position of the benzamide moiety with small electron-withdrawing substituents (namely fluorine) as well as by substitution with alkyl carboxamide / aryl carboxamide/ phenyl/ aryl amine functions at the pyrazine scaffold (**Figure 4**).

As **CI-994** contains -$NHCOCH_3$ group, initially it was tried in both these positions (R^1 and R^2). Then, the effect of NHCOPh was taken into consideration whether bulkier substitution was better or not. Finally, phenyl, aminophenyl and aminobenzyl substitutions were tried at these R^1 and R^2 positions to judge or compare their efficacy with respect to the earlier ones. As there is no compounds of such type reported earlier combining scaffolds of these two prototype compounds (**CI-994** and **BG-45**), these groups (alkyl carboxamide / aryl carboxamide/ phenyl/ aryl amine functions) were chosen particularly at these R^1 and R^2 positions to get an initial idea that which type of substituents was preferable at these positions to synthesize newer better active molecules.

2.2. Chemistry

Scheme 1 outlines the synthesis of an intermediate; *tert*-butyl (2-aminophenyl) carbamate (**2**). Here *o*-phenylenediamine (**1**) was protected at one amino group using di-*tert*-butyl dicarbonate.

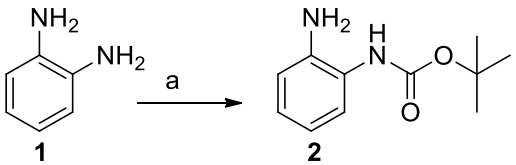

Scheme 1. *Reagent and conditions*: (a) di-tert-butyl dicarbonate, triethylamine, ethanol, RT, 5h.

Scheme 2 represents the synthesis of an intermediate *tert*-butyl (2-amino-5-fluorophenyl) carbamate (**6**). The reaction started with boc protection of 5-fluro-2-nitroaniline (**3**) which yielded the compound (**4**) with diprotection at the amino group. This compound (**4**) was selectively deprotected with controlled condition using trifluoroacetic acid gave monoprotected amino group (**5**) (44). Compound **5** upon catalytic hydrogenation with Pd/C produced compound **6** which was further utilized as an intermediate for synthesis of the final compounds.

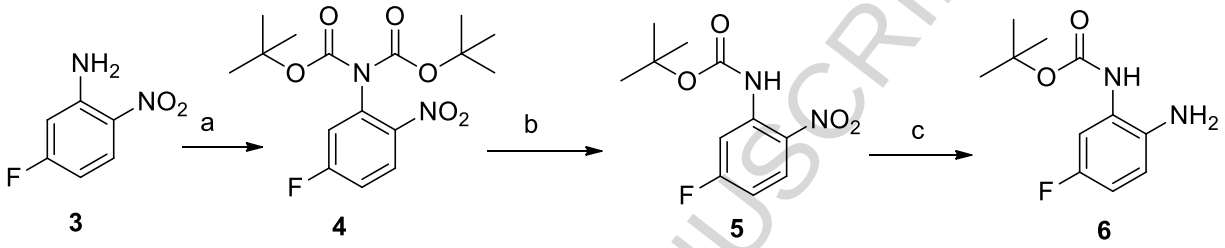

Scheme 2. *Reagent and conditions*: (a) di-tert-butyl-dicarbonate, DMAP, 2-methyl THF, RT, 12h (b) trifluoroacetic acid(3%), DCM, RT, 2 h (c) Pd/C, H_2balloon, Methanol, RT, 4h

Scheme 3 illustrates the synthetic route of final molecules (compound **12a**, **12b**, **12c** and**12d**). Here, methyl 5-(chloropyrazine)-2-carboxylate (**7**) was first converted to methyl 5-(aminopyrazine)-2-carboxylate (**8**) using sodium azide and triphenylphosphene (45). Here, substituted chloropyrazine got converted to substituted azidopyrazine using sodium azide which also isomerizes to its tetrazolo form *in situ*. The azidopyrazine forms iminophosphorane in the presence of triphenylphosphene which gets hydrolyzed to amine under acidic condition, a typical Staudinger reaction (46). *N*-acetylation of methyl 5-(aminopyrazine)-2-carboxylate (**8**) yielded compound **9a** while *N*-benzoylation produced compound **9b**. These intermediates were hydrolyzed to their acid derivatives compound **10a** and compound **10b**, and were coupled with **2** and **6** to get **11a**, **11b**, **11c** and **11d**. Deprotection of the compounds afforded final compounds **12a**, **12b**, **12c**, **12d**.

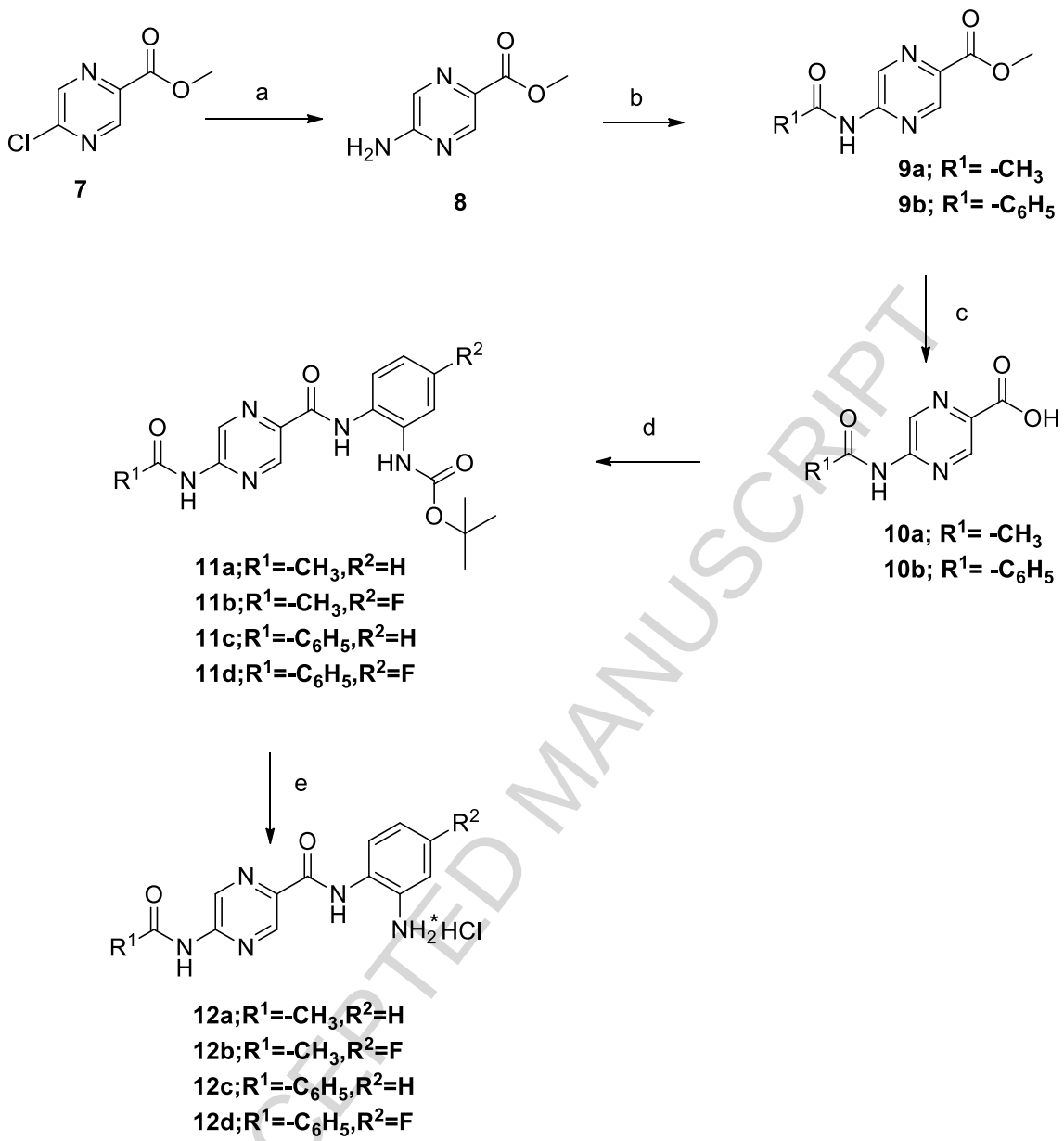

Scheme 3. *Reagent and conditions*: (a) i. sodium azide, triphenylphosphene, dimethyl sulphoxide, 120^{o}C, 4h ii. 1N HCl, 120^{o}C, 2h iii. $NaHCO_3$ (b) i. acetic anhydride, 90^{o}C, 2h ii. benzoyl chloride, sodium hydride, DMF, 0°C, 5 h (c) lithium hydroxide, THF:water (3:1), RT, 3h (d) compd. **2** or compd. **6**, EDC, DMAP, DCM:pyridine (1:1), RT, 12h (e) 4M HCl in dioxane, DCM, 0^{o}C, 2h.

Scheme 4 discusses the synthesis of target molecules**18a** and **18b** which mimics scheme 3 in mechanisms with difference of methyl 6-(chloropyrazine)-2-carboxylate (**13**) instead of methyl 5-(chloropyrazine)-2-carboxylate (**7**).

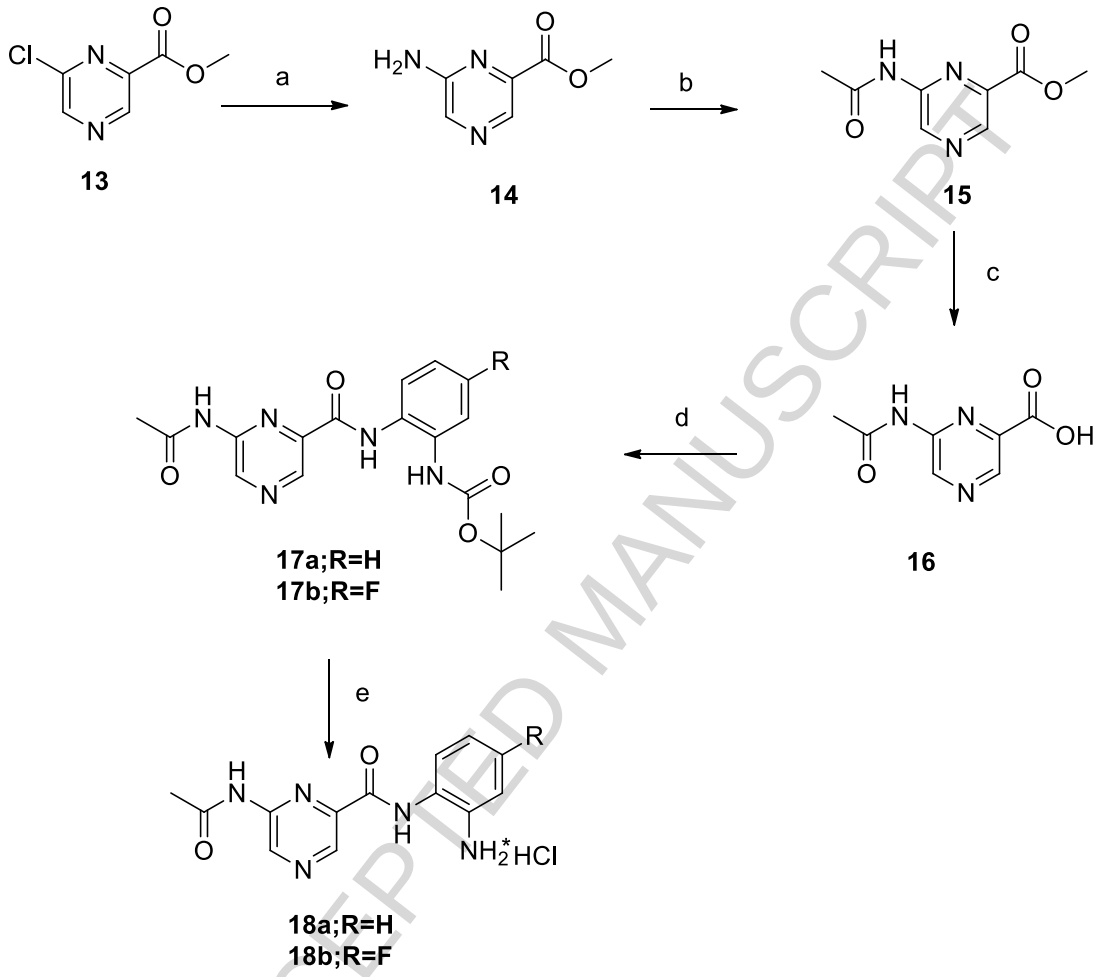

Scheme 4. *Reagent and conditions*: (a) i. sodium azide, triphenylphosphene, dimethyl sulphoxide, 120^{o}C, 4h ii. 1N HCl, 120^{o}C, 2h, iii. $NaHCO_3$ (b) acetic anhydride, 90^{o}C, 2h (c) lithium hydroxide, THF:water (3:1), RT, 3h (d) compounds **2** or **6**, EDC, DMAP, DCM:pyridine (1:1),RT, 12h (e) 4M HCl in dioxane, DCM, 0^{o}C, 2h

Scheme 5 shows the synthesis of target molecules **22a** and **22b**. The first reaction describes Suzuki coupling where methyl 5-(chloropyrazine)-2-carboxylate (**7**) was reacted with phenyl

boronic acid in presence of bis(triphenylphosphine)palladium(II)dichloride as a catalyst and potassium carbonate using 1,4-dioxane solvent to get compound **19**. This compound (**19**) on alkaline hydrolysis formed its acid derivative **20**. This was coupled with intermediates **2** and **6** by EDC catalyzed acid-amine coupling to get **21a** and **21b** which upon boc deprotection by acid made final products **22a** and **22b** respectively.

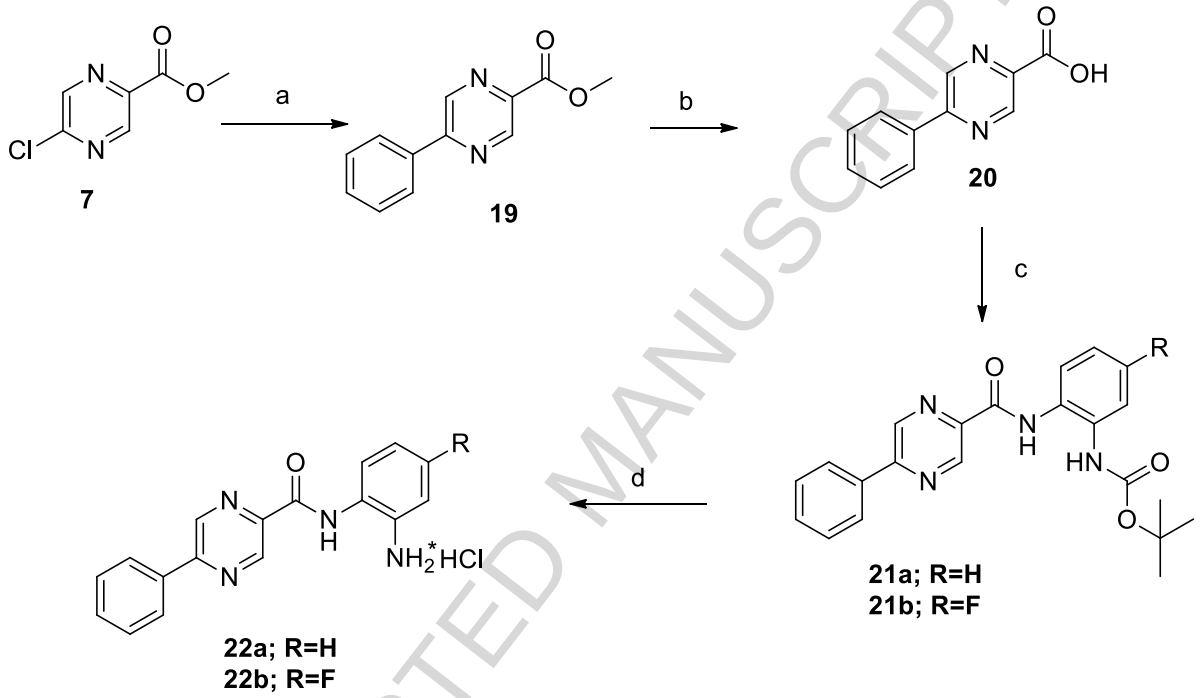

Scheme 5. *Reagent and conditions*: (a) phenyl boronic acid, bis (triphenylphosphine) palladium(II) dichloride, potassium carbonate, 1,4-dioxane, 100^{o}C, 12h (b) lithium hydroxide, THF: Water (3:1), RT, 3h (c) 2 or 6, EDC, DMAP, DCM:pyridine (1:1), RT, 12h (d) 4M HCl in dioxane, DCM, 0^{o}C, 2h.

Scheme 6 depicts synthesis of target molecules **26a**, **26b**, **26c** and **26d.** Methyl 5-(chloro pyrazine)-2-carboxylate (**7**) was reacted with aniline or benzylamine in presence of *p*-toluene sulphonic acid and respective amines (compound **23a**, **23b**) were prepared. These compounds on

alkaline hydrolysis formed respective acids (compound **24a**, **24b**). These were coupled with intermediate compounds **2** and **6** by EDC catalyzed acid-amine coupling to get compounds **25a**, **25b**, **25c**, **25d** which upon deprotection by acid made final products **26a**, **26b**, **26c** and **26d**.

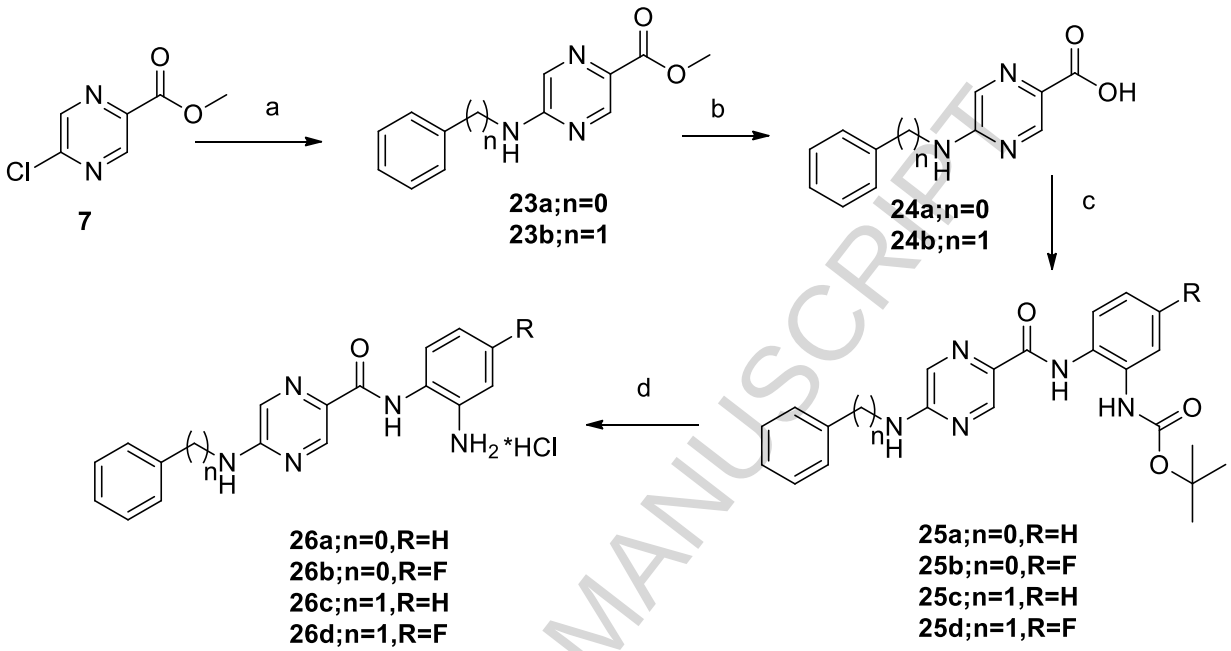

Scheme 6. *Reagent and conditions* (a) aniline (n=0) or benzylamine (n=1), p-toluenesulphonic acid, 1,4-dioxane, 100^{o}C,12h (b) lithium hydroxide, THF:water (3:1), RT, 3h (c) compound **2** or compound **6**, EDC, DMAP, DCM:pyridine (1:1), RT, 12h (d) 4M HCl in dioxane, DCM, 0^{o}C, 2h.

Purity of these final compounds was evaluated using ^{1}H NMR, ^{13}C NMR and LC-MS analysis. Spectral data of these final compounds are provided in the supplementary materials (Text S1).

2.3. Pan HDAC inhibition assay using HeLa nuclear extract

The target compounds were screened for their HDAC inhibitory activity using *color de lys*® HDAC assay kit (BML-AK501, ENZO life sciences). **CI-994** and **BG45** are used as positive

controls for the assay. HeLa nuclear extract (expresses HDAC1 and HDAC2 dominantly) (47) was used as a source of HDAC activity. The results are summarized in **Table 1**.

Table 1. HDAC inhibitory data of target compounds

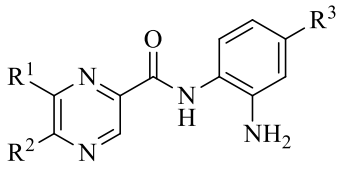

Cpd[a]	R^1	R^2	R^3	% inhibition in HeLa nuclear extract (at 5 µM)	% inhibition in HDAC3 assay (at 1 µM)
12a	H	$CONHCH_3$	H	59.6	43.54
12b	H	$CONHCH_3$	F	64.1	39.04
12c	H	NHCOPh	H	57.1	44.70
12d	H	NHCOPh	F	57.6	28.60
18a	$CONHCH_3$	H	H	48.6	29.27
18b	$CONHCH_3$	H	F	50.4	38.70
22a	H	Ph	H	35.47	32.11
22b	H	Ph	F	29.27	22.24
26a	H	NHPh	H	63.9	40.24
26b	H	NHPh	F	71.5	67.48
26c	H	NHBnz	H	65.6	62.24
26d	H	NHBnz	F	65.0	59.04
CI-994	--	--	--	53.8	53.65
BG45	H	H	H	55.4	57.97

[a] Compound number

All compounds were found to exhibit HDAC enzyme inhibition at 5µM in duplicate. Compounds **26b**, **26c** and **26d** demonstrated an increased HDAC inhibition compared to **CI-994** and **BG45**. These compounds were screened for determination of IC_{50} of enzyme inhibition along with **CI-994** and **BG45.** Compound **26b**, **26c** and **26d** (IC_{50}= 1.972±2.18 µM, 2.869±1.36 µM and 3.072±1.56 µM, respectively) showed more promising HDAC inhibitory efficacy compared to **CI-994** (IC_{50}= 5.369±0.78 µM) and **BG-45** (IC_{50}= 5.506±1.21 µM) (**Table 2**) and **(Figure-5 A and B)**.

Table 2. IC_{50} values of promising compounds and their selectivity profile

Cpd[a]	IC_{50} (μM)		Selectivity for HDAC3 (Pan HDAC/HDAC3)
	HeLa nuclear extract (Pan HDAC inhibition)	HDAC3	
26b	1.972	0.335	5.87
26c	2.869	0.245	11.68
26d	3.072	0.540	5.68
CI-994	5.369	0.917	5.85
BG45	5.506	0.558	9.87

[a] Compound number

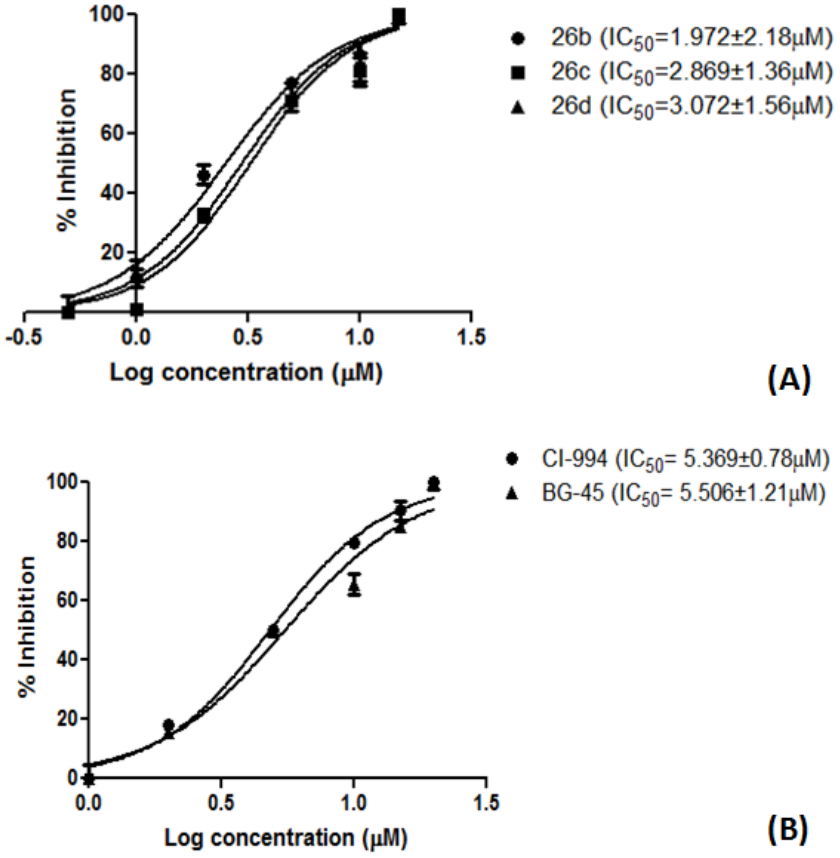

Figure 5. IC_{50} determination of HDAC enzyme inhibition using HeLa nuclear extract for compound **26b, 26c** and **26d** [A] and **BG-45** and **CI-994** [B]. The data represents mean ± SD (n=2).

2.4. HDAC3 inhibition assay using recombinant HDAC3/NCOR1

Target compounds were evaluated for their inhibition potency towards HDAC3 enzyme using HDAC3/NCOR1 fluorometric drug discovery kit (BML-AK531, ENZO life sciences). All these compounds showed more inhibition of HDAC3 activity compared to nuclear extract (**Table 1**). For better understanding, the most potent HDAC3 inhibitor compounds **26b**, **26c** and **26d** (67.48%, 62.24% and 59.04% respectively with 1µM compound concentration in duplicate) were further evaluated for their IC_{50} values along with **CI-994** and **BG45** as positive control (**Table 2**, **Figure 6 A and B).** Compound **26b, 26c, 26d**, **BG-45** and **CI-994** were evaluated for IC_{50} determination. It was observed that the selected compounds were more effective than **CI-994** and **BG-45**. Compound **26c** appeared to be as a lead in the series having the highest HDAC3 inhibition (IC_{50} = 0.245 µM) with ~12 fold HDAC3 selectivity over Pan HDACs.

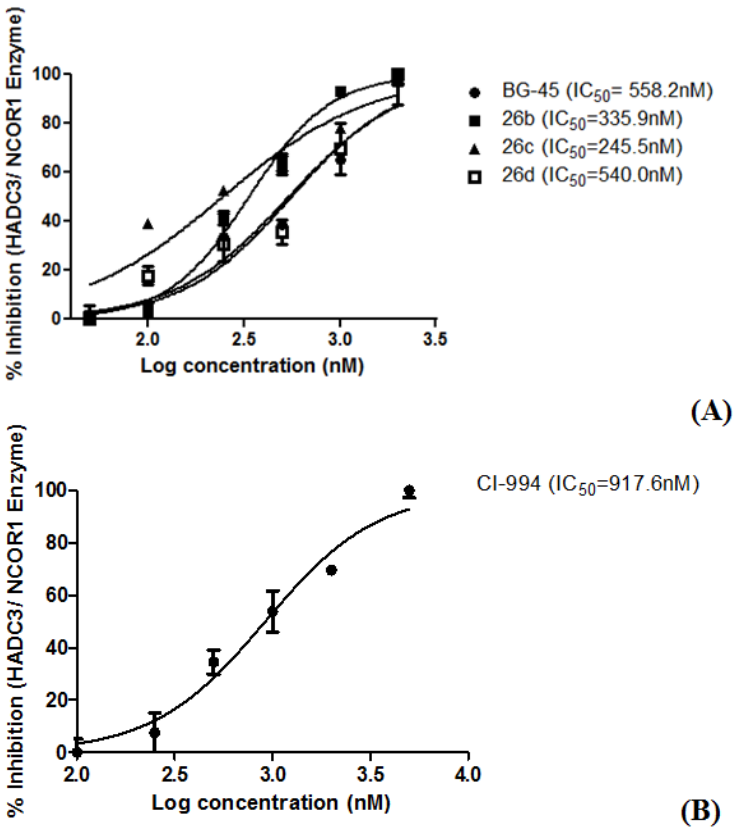

Figure 6. IC_{50} determination of HDAC3 enzyme inhibition using recombinant HDAC3/NCOR1 complex for compound **26b, 26c** and **26d** and **BG-45** [A] and **CI-994** [B]. The data represents mean ± SD (n=2).

Some interesting relationship between the structures of the synthesized molecules and their biological activity came out from the study. Incorporating fluoro substitution at the *para* position of the benzamide moiety at compound **12a** resulted in lower Hela nuclear extract inhibition than compound **12b**. However, compound **12a** showed slightly lower HDAC3 inhibition (39.04%) compared to compound **12a** (43.54%). Again, the corresponding methyl carboxamide substitution at R^1 position instead of R^2 position led to a decreased Hela nuclear extract inhibition that strongly suggested that R^2 substituents (such as $CONHCH_3$) were not preferable than the corresponding R^1 substituents (compound **12a** *vs* compound **18a**; compound **12b** *vs*

compound **18b**) as far as the HeLa nuclear extract inhibition was concerned. However, $CONHCH_3$ substitution at R^2 position yielded better HDAC3 inhibitors (compound **12a** *vs* compound **18a**; compound **12b** *vs* compound **18b**). Hence, further structural modification was performed at R^2 position to judge the activity trend. Incorporation of phenyl group at the terminal end of amino carbonyl moiety did not improve HeLa nuclear extract inhibition rather showed decrease activity (compound **12a** *vs* compound **12c**; compound **12b** *vs* compound **12d**). However, these compounds also displayed lower (compound **12b** *vs* compound **12d**) or comparable (compound **12a** *vs* compound **12c)** HDAC3 inhibitory activity. Therefore, the carbonyl function has been withdrawn from the next design. Incorporation of bulky phenyl ring at R^2 decreased both the HeLa nuclear extract inhibitory and HDAC3 inhibitory properties (compound **22a** *vs* compound **12a**). The structure was further modified with the introduction of aryl amine function at R^2 position which yielded compounds with comparable HDAC3 inhibitory efficacy (compound **26a** *vs* compound **12a**). However, both higher HeLa nuclear inhibitory and HDAC3 inhibitory activities were observed for the corresponding *p*-fluoro analogs (compound **26b** *vs* compound **12b**). Additionally, incorporation of a methylene spacer between the aryl (phenyl) and amine nitrogen resulted in both comparable HeLa nuclear inhibition and HDAC3 inhibition (compound **26c** and **26d**). Moreover, it was noticed that for both HeLa nuclear inhibitory activity and HDAC3 inhibitory activity, arylamine groups (NHPh and NHBnz) at R^2 position were better effective than the corresponding phenyl groups (compounds **26a**-**26d** vs compounds **22a**-**22b**). Therefore, it may be assumed that not only the steric or hydrophobic effect at R^2 position (phenyl or benzyl) is necessary but also the presence of associated amino function is crucial for imparting higher inhibitory effects. The overall approach of derivatization of **BG-45** and **CI-994** resulted in the identification of compound **26c** with 11.68-fold HDAC3

selectivity over pan-HDAC (**BG-45**; 9.9-fold and **CI-994**; 5.85-fold). In a nutshell, it may be inferred that aminobenzyl or aminophenyl group at R^2 position is better effective than the phenyl, methylcarboxamido (NHCOMe) or methylaminocarbonyl (CONHMe) functions at the same position.

2.5. Antiproliferative assay using cancer cell lines

Cytotoxicity studies were performed on two different cell lines, i.e., B16F10 (murine melanoma cell line) and HeLa (Human cervical cancer cell line) by MTT assay method. All the synthesized compounds were evaluated at two different concentrations (100 μM and 10 μM) in triplicate. **CI-994** and **BG45** were taken as the standard reference compounds in the assay **(Supplementary Figure S1).** From the assay results, it was observed that majority of the compounds displayed good cytotoxicity on both the cell lines. Compounds **12a**, **22a**, **26a**, **26c** and **26d** were found to be more promising and these were further subjected to evaluate for their 50% inhibitory concentration (IC_{50}) with a wider of concentrations. The cell viability after 72 hours of treatment was measured by MTT assay (**Figure 7**).

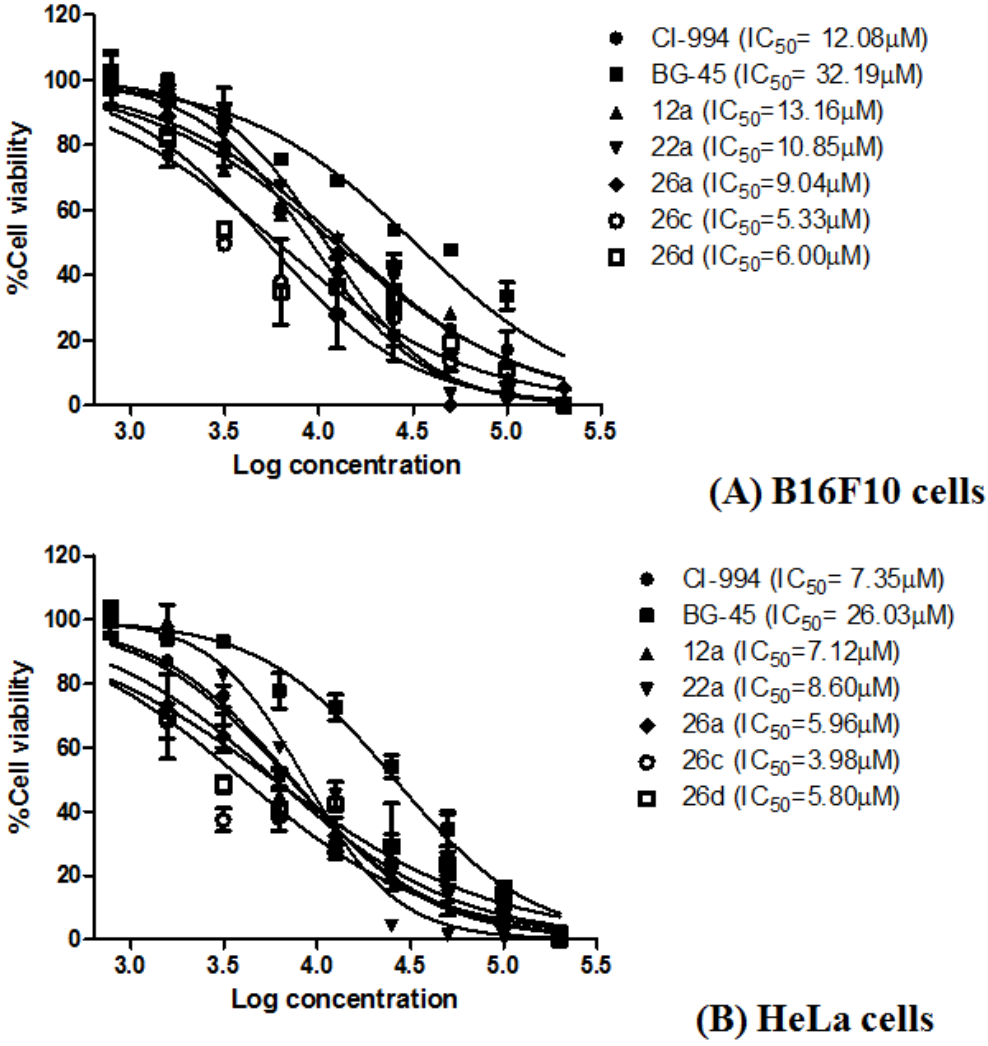

Figure 7. Dose response curve and IC_{50} values of promising compounds **12a**, **22a**, **26a**, **26c** and **26d** along with **BG-45** and **CI-994**. All compounds were explored in larger range of nine different concentrations on B16F10 (A) and HeLa (B) cells. Cells were treated with compounds for 72 hours and cell viability was measured by *in vitro* MTT assay method. Data represents mean ± SD (n=2) and plotted in dose response format. IC_{50} was calculated using nonlinear regression analysis method using Graph Pad Prism5.

Most of the selected compounds exhibited better cytotoxicity compared to **CI-994** and **BG45**. Interestingly compound **12a** containing the molecular structural information of both **BG45** and

CI-994 exhibited similar efficacy compared to **CI-994** but more efficacious than **BG45** in both the B16F10 and HeLa cell lines (**Figure 7**). Compound **26c** (IC_{50} of 5.33 μM in B16F10 cells and 3.99 μM in HeLa cells) and compound **26d** (IC_{50} of 6.00 μM in B16F10 cells and 5.80 μM in HeLa cells) were found to be the most potent among these compounds and therefore, these compounds (compounds **26c** and **26d**) were further carried over for other biological assays.

2.6. Apoptosis assay

The extent of apoptosis induced by novel molecules (compounds **26c** and **26d**) was determined by using Annexin V FITC/PI dead cell detection kit using B16F10 cells. HDAC inhibitors induce apoptosis which results in cell death by altering gene expression (48). The percentage apoptosis induced by target compounds **26c** and **26d** was investigated in the experiment along with **CI-994** and **BG45** (**Figure 8**).

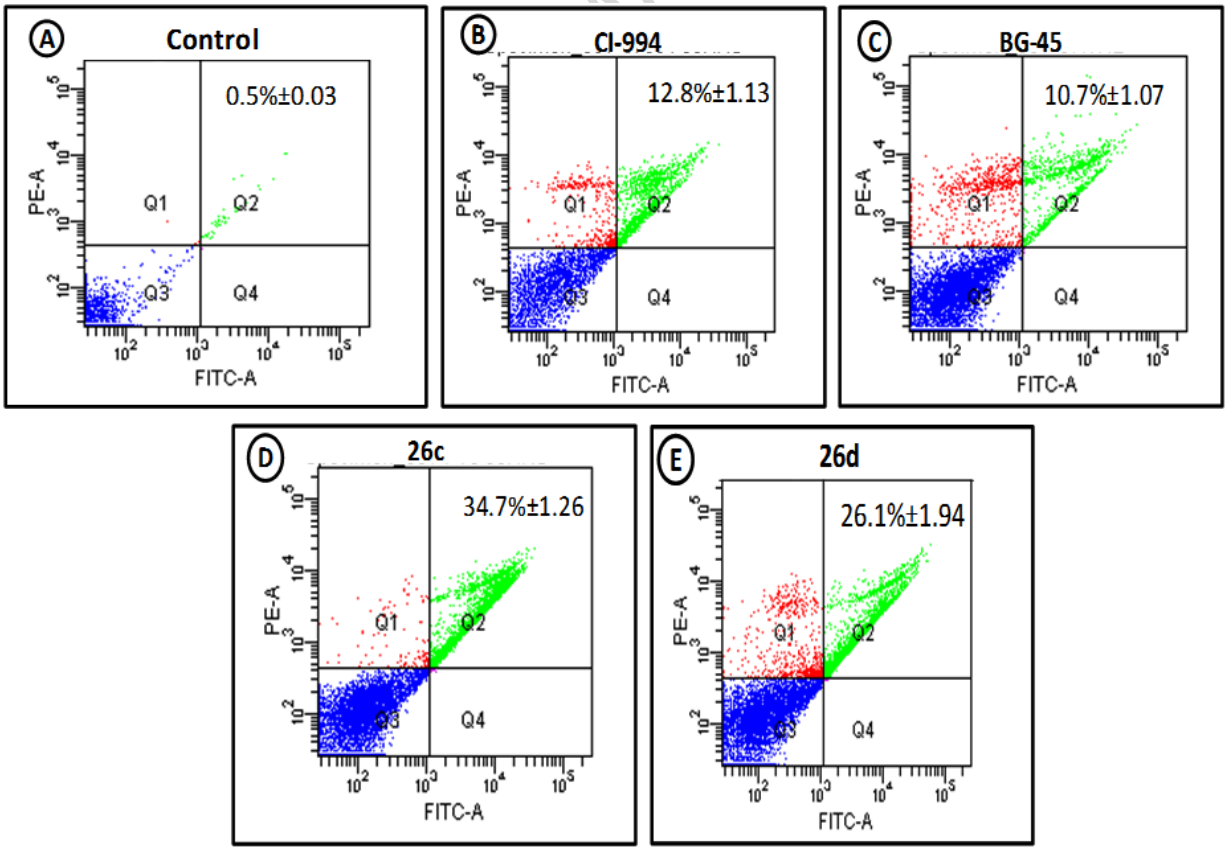

Figure 8. Induction of apoptosis in B16F10 cells quantified by Annexin V/PI assay using flow cytometry. (A) **Control** (B) **CI-994** (C) **BG45** (D) **26c** (E) **26d**. [Q2 quadrant depicts late apoptosis and Q4 quadrant shows early apoptosis. X-axis: Annexin-V intensity, Y-axis: propidium iodide intensity.

Results displayed (**Figure 8**) that 10.7±1.07% and 12.8±1.07% cells were present in late apoptotic phase (Q2) for **BG45** and **CI-994** respectively. For compound **26d**, 26.1±1.94% cells were present in Q2 quadrant demonstrated more effective while the highest apoptosis was exhibited by compound **26c** showing 34.7±1.26% cells in the late apoptotic phase [Q2]. The experiment proved an enhanced efficacy of the novel synthesized lead derivatives compared to **CI-994** and **BG45**.

2.7. Cell cycle analysis

We further investigated the effect of **26c** and **26d** on cell cycle progression in B16F10 cells (**Figure 9**). From the result, it was found that compound **26c** and **26d** induced growth arrest at G2/M phase of cell growth. Compound **26c** induced significant growth arrest around 43.7% in G2/M phase compared to control showing 9.32%, while G0/G1 phase decreased to 11.6% from 74.6%. The similar pattern of growth arrest was found for **26d** and **BG-45** also. While **CI-994** induced cell arrest in G0/G1 phase of cell cycle was 82.3%. These results indicated that compound **26c** might produce anticancer activity with the growth arrests at G2/M phase.

[A] Control

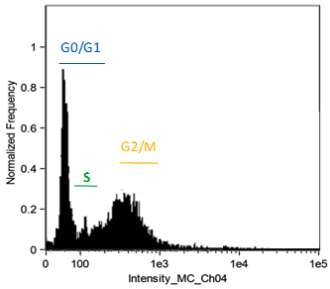

G0/G1	74.6
S	2.71
G2/M	9.32

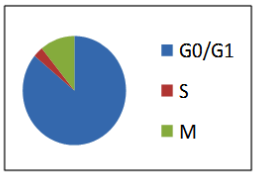

[B] Cl-994

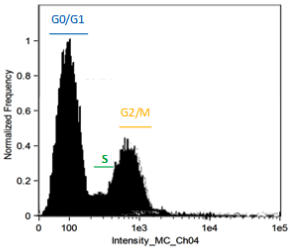

G0/G1	82.3
S	4.01
G2/M	15.5

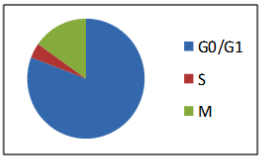

[C] BG 45

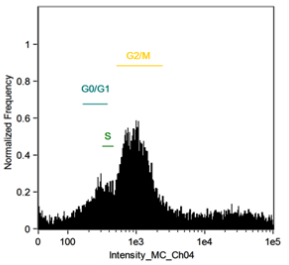

G0/G1	9.32
S	4.71
G2/M	35.5

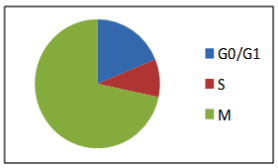

[D] 26c

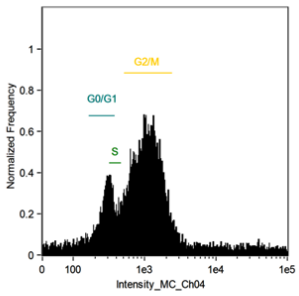

G0/G1	11.6
S	6.09
G2/M	43.7

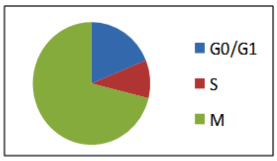

[E] 26d

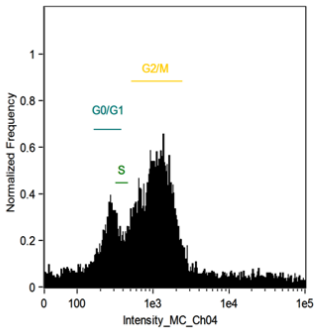

G0/G1	12.6
S	5.3
G2/M	39.7

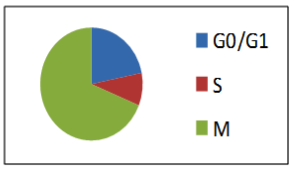

Figure 9. Cell cycle arrest induced in B16F10 cells by (A) **control**, (B) **CI-994**, (C) **BG-45**, (D) **26c**, (E) **26d**.

3. Conclusion

Here, we have designed and synthesized a series of 2-aminobenzamide derivatives as selective HDAC3 inhibitors. All target compounds were evaluated for their HDAC enzyme inhibition efficiency with HeLa nuclear extract and recombinant HDAC3 enzyme and these compounds were found to be effective HDAC inhibitors with preferential selectivity for HDAC3. These compounds were also tested for their antiproliferative activity in two different cell lines (B16F10 and HeLa). Compound **26c** exhibited potent cell growth inhibition compared to both **CI-994** and **BG45**. One of the lead compound (compound **26c**) showed appreciable selectivity (11.68-fold) in HDAC3 inhibition over pan HDACs which is quite significant than **CI-994** (5.85-fold) and **BG-45** (9.9-fold). Compound **26c** induced significant cell growth arrest in G2/M phase and increased apoptosis level indicating improved anticancer potential compared to **CI-994** and **BG45**. Overall effort to make potent and selective HDAC inhibitors with different structural medication on the overlapping backbone of **BG45** and **CI-994** resulted in compound **26c** as a potential HDAC3 inhibitor. Additionally, all these biological evaluation studies indicated compound **26c** can be further explored as a promising compound for anticancer therapy.

4. Experimental

4.1. Chemistry

All starting materials and reagents were commercially available and used without further purification. All reactions were monitored by thin layer chromatography (TLC) using precoated

plates with silica gel F254 from Merck Millipore Co., USA. ^{1}H and ^{13}C NMR spectrum were recorded in DMSO-d_6 and $CDCl_3$ using Bruker-400 MHz and chemical shifts reported in ppm using tetramethylsilane as internal standard. Mass spectroscopy was performed in LCMS-2020, Schimadzu using ESI mode. The Purity of the compounds were analyzed by Analytical LC/MS. Analysis was performed on a LCMS-8040 equipped with a photodiode array detector using a Shiseido C18 4.6×150 mm, 5µ column at a flow rate of 1 mL/min with isocratic flow (50% A: 50% B for compound **12a, 12b, 18a** and **18b** while for rest of the compounds it was 65%A: 35%B; Solvent A = water, solvent B = methanol).

4.1.1. Preparation of *tert*-butyl (2-aminophenyl)carbamate (2)

o-Phenylenediamine (5g, 0.0462mmol) was dissolved in 20 mL ethanol and triethylamine (7.01g, 0.0693mmol) was added. The mixture was stirred in ice bath for 20 minutes. Di-*tert*-butyl dicarbonate (10.09g, 0.04623mmol) was mixed with 10 mL of ethanol and added slowly to stirring reaction mixture and stirred for 5 hours at ambient temperature. The solvent was evaporated and the residue was fractioned between ethyl acetate and water. The ethyl acetate layer was evaporated and crude mixture was purified using column chromatography (EtOAc:Hexane;1:9) to give 6.5 g (yield 67.7 %) of **2** as white solid. ^{1}H NMR (400 MHz, DMSO-d_6) δ 8.29 (s, 1H), 7.17 (d, *J* = 7.6 Hz, 1H), 6.83 (t, *J* = 7.6 Hz, 1H), 6.67 (dd, *J*= 7.9, 1.3 Hz, 1H), 6.54 – 6.49 (m, 1H), 4.82 (s, 2H), 1.45 (s, 10H). $C_{11}H_{16}N_2O_2$ [M]: 208.26; MS (ESI) *m/z*: $[M+H]^+$: 209.10 $[M-H]^+$: 207.10

4.1.2. Di boc protection of 5-fluoro 2-nitro aniline as compound 4

5-fluoro-2-nitroaniline (**3**) (4g, 0.0256 mmol) was dissolved in 2-methyl THF (40 mL) and 4-dimethyl amino pyridine (62mg, 0.0005mmol) was added. The reaction mixture was cooled at 0°C, di-tert-butyl dicarbonate (11.18g, 0.05124 mmol) was added drop wise and stirred at room

temperature for 12 hours. Solvent was evaporated and crude was fractioned between water and EtOAc, dried over Na_2SO_4 and concentrated. The crude mixture was purified using column chromatography (EtOAc: Hexane; 0.1:9.9) to yield intermediate **4** as yellow solid 5.2 g (yield 69%).^{1}H NMR (400 MHz, $CDCl_3$) δ 8.15 (dd, *J* = 9.1, 5.5 Hz, 1H), 7.24 – 7.15 (m, 1H), 7.06 (dd, *J* = 8.3, 2.6 Hz, 1H), 1.42 (s, 18H). $C_{16}H_{21}FN_2O_6$ [M]: 356.35; MS (ESI) *m/z*: $[M+Na]^+$: 379.10

4.1.3. Preparation of *tert*-butyl (5-fluro-2-nitrophenyl) carbamate (5)

Compound **4** (5g, 0.0104mmol) was dissolved in 50 mL of DCM and cooled in an ice bath. Trifluoro acetic acid (1.5mL) was added and stirred for 2 hours. Dichloromethane was evaporated and the mixture was neutralized with sodium bicarbonate solution. Product was extracted in ethyl acetate. Organic layer was concentrated to yield 3.47 g of compound **5** as yellow solid (yield 96.6%). ^{1}H NMR (400 MHz, $CDCl_3$) δ 9.89 (s, 1H), 8.40 (dd, *J* = 11.6, 2.6 Hz, 1H), 8.26 (dd, *J* = 9.4, 5.9 Hz, 1H), 6.78 (m, 1H), 1.55 (s, 9H). $C_{11}H_{13}FN_2O_4$ [M]: 256.23; MS (ESI) *m/z*: $[M-H]^+$: 255.10

4.1.4. Preparation of *tert*-butyl (2-amino-5-fluorophenyl)carbamate (6)

Compound **5** (3.4g, 0.0132mmol) was mixed with 40 mL methanol and a catalytic amount of 10% Pd/C was added. Hydrogen gas was supplied through hydrogen balloon and the reaction was stirred for 4 hours. The reaction mixture was filtered through the bed of celite® and filtrate was evaporated to get 2.9 g of compound **6** as brown solid. (yield 96.6%). ^{1}H NMR (400 MHz, DMSO-d_6) δ 8.42 (s, 1H), 7.20 (d, *J* = 10.9 Hz, 1H), 6.66 (dd, *J* = 6.9, 1.5 Hz, 2H), 4.78 (s, 2H), 1.47 (s, 10H). $C_{11}H_{15}FN_2O_2$ [M]: 226.25; MS (ESI) *m/z*:: $[M-H]^+$:225.10

4.1.5. Preparation of methyl 5-aminopyrazine-2-carboxylate (8)

Methyl 5-(chloropyrazine)-2-carboxylate (**7**) (2 g, 0.0115mmol) was dissolved in 80 mL of DMSO. Sodium azide (3 g, 0.0463mmol) and triphenylphosphene (4.6 g, 0.1738mmol) were added and the mixture was refluxed at 120°C for 4 hours. 20 mL of 1N HCl was added and the reaction was continued at 120°C for 2 hours. The mixture was cooled and neutralized by aqueous $NaHCO_3$ solution and product was extracted in ethyl acetate, dried using Na_2SO_4. The ethyl acetate fraction was evaporated and washed with n-pentane to get 0.7 g (yield 39.5%) yellow solid of compound **8**.^{1}H NMR (400 MHz, DMSO-d_6) δ 8.53 (d, *J* = 1.2 Hz, 1H), 7.91 (d, *J* = 1.2 Hz, 1H), 7.39 (s, 2H), 3.79 (s, 3H). $C_6H_7N_3O_2$ [M]: 153.14; MS (ESI) *m/z*: $[M-H]^+$: 152.05

4.1.6. Preparation of methyl 5-acetamidopyrazine-2-carboxylate (9a)

Methyl 5-aminopyrazine-2-carboxylate (**8**) (0.650g, 4.2483mmol) was reacted with excess of acetic anhydride (5mL) and heated at 90°C for 2 hours. The reaction mixture was evaporated and partitioned between saturated $NaHCO_3$ solution and ethyl acetate. Organic layer was evaporated to get 0.345g of compound **9a** as pale yellow solid (yield 41.6%). ^{1}H NMR (400 MHz, DMSO-d_6) δ 11.29 (s, 1H), 9.41 (d, *J* = 1.4 Hz, 1H), 8.96 (d, *J* = 1.4 Hz, 1H), 2.18 (s, 3H), 1.81 (s, 3H). $C_8H_9N_3O_3$ [M]: 195.18; MS (ESI) *m/z*: $[M+H]^+$: 196.05 $[M-H]^+$, 194.05

4.1.7. Preparation of methyl 5-benzamidopyrazine-2-carboxylate (9b)

Methyl 5-aminopyrazine-2-carboxylate (**8**) (0.250g, 1.6339mmol) was dissolved in 5 mL of DMF. Sodium hydride (0.118g, 4.9017mmol) was added to above mixture and stirred in ice bath for 30 minutes. Benzoyl chloride (0.230g, 1.6339mmol) was added and stirred for 12 hours. Reaction mixture was poured in a beaker containing ice and slowly aqueous ammonium chloride solution was added. Product was extracted in ethyl acetate and evaporated ethyl acetate fraction was purified by column chromatography (EtOAc:Hexane; 3:7) to get 0.3 g of compound **9b** as

white fluffy solid (yield 70.62%).^{1}H NMR (400 MHz, DMSO-d_6) δ 11.60 (s, 1H), 9.55 (d, *J* = 1.4 Hz, 1H), 9.05 (d, *J* = 1.4 Hz, 1H), 8.09 – 8.05 (m, 2H), 7.66 (t, *J* = 7.4 Hz, 1H), 7.56 (t, *J* = 7.6 Hz, 2H), 3.92 (s, 3H). $C_{13}H_{11}N_3O_3$ [M]: 257.24; MS (ESI) *m/z*: $[M+H]^+$: 258.05 $[M-H]^+$, 256.05

4.1.8. Procedure A: Preparation of 5-acetamidopyrazine-2-carboxylic acid (10a)

Compound **9a** (0.334g, 1.7641mmol) was added in THF and stirred for 30 minutes. Lithium hydroxide (0.081g, 3.5282mmol) was dissolved in water and added to the above mixture and stirred overnight. It was neutralized with dil. HCl and extracted in ethyl acetate, dried and concentrated to get 0.220g of 1**0a** as white solid(yield 69%) and it was sufficiently pure to use as a starting material for the successive step. ^{1}H NMR (400 MHz, DMSO-d_6) δ 11.19 (s, 1H), 9.40 (s, 1H), 8.94 (s, 1H), 2.18 (s, 3H). $C_7H_7N_3O_3$ [M]: 181.05; MS (ESI) *m/z*: $[M-H]^+$: 180.05

4.1.9. Preparation of 5-benzamidopyrazine-2-carboxylic acid (10b)

This compound was also prepared by following method A form compound **9b** (0.3g, 1.1673 mmol) to obtain 0.183g of pale yellow solid (yield 64.5%). ^{1}H NMR (400 MHz, DMSO-d_6) δ 13.53 (s, 1H), 11.55 (s, 1H), 9.54 (d, *J* = 1.4 Hz, 1H), 9.03 (d, *J* = 1.4 Hz, 1H), 8.10 – 8.05 (m, 2H), 7.68 – 7.63 (m, 1H), 7.56 (t, *J* = 7.6 Hz, 2H). $C_{12}H_9N_3O_3$ [M]: 243.22; MS (ESI) *m/z*: $[M-H]^+$: 242.05

4.1.10. Procedure B: Preparation of *tert*-butyl (2-(5-acetamidopyrazine-2-carboxamido) phenyl) carbamate (11a)

Compound **10a** (0.2g, 1.0256mmol) was dissolved in a mixture of DCM: Pyridine (1:1). 1-(3-Dimethylaminopropyl)-3-ethylcarbodiimide hydrochloride (0.294g, 1.5384mmol) and catalytic amount of 4-(dimethylamino) pyridine (DMAP) were added to the reaction mixture. *tert*-butyl (2-aminophenyl) carbamate (**2**) (0.234g, 1.1281mmol) was added and reaction was flushed with

nitrogen gas. The reaction mixture was stirred for 12 hours at room temperature to complete reaction. The solvent was evaporated and product was fractioned between ethyl acetate and saturated solution of sodium bicarbonate. The crude product was purified by column chromatography (EtOAc: Hexane; 2.5:7.5),afforded 0.150g of compound **11a** as a cream powder (yield 37%).^{1}H NMR (400 MHz, DMSO-d_6) δ 11.26 (s, 1H), 10.27 (s, 1H), 9.35 (d, *J* = 1.0 Hz, 1H), 9.04 (d, *J* = 1.2 Hz, 1H), 7.93 (d, *J* = 8.6 Hz, 1H), 7.30 – 7.15 (m, 4H), 2.19 (s, 3H), 1.50 (s, 9H). $C_{18}H_{21}N_5O_4$ [M]: 371.39; MS (ESI) *m/z*: $[M+H]^+$: 372.10 $[M-H]^+$, 370.15

4.1.11. Preparation of *tert*-butyl (2-(5-acetamidopyrazine-2-carboxamido)-5-fluoro phenyl) carbamate (11b)

Following procedure B, compound **11b** was synthesized from **10a** (0.150g, 0.8333mmol) and compound **6** (0.189g, 0.8333mmol) as pale pink powder (0.070g, yield 22%). ^{1}H NMR (400 MHz, DMSO-d_6) δ 11.25 (s, 1H), 10.25 (s, 1H), 9.37 (d, *J* = 1.4 Hz, 1H), 9.22 (s, 1H), 9.02 (d, *J* = 1.4 Hz, 1H), 7.77 (dd, *J* = 9.0, 6.1 Hz, 1H), 7.27 (dd, *J* = 10.4, 2.9 Hz, 1H), 7.10 – 7.05 (m, 1H), 2.19 (s, 3H), 1.49 (s, 9H). $C_{18}H_{20}FN_5O_4$ [M]: 389.38; MS (ESI) *m/z*: $[M+H]^+$: 390.15 $[M-H]^+$, 388.20

4.1.12. Preparation of *tert*-butyl (2-(5-benzamidopyrazine-2-carboxamido) phenyl) carbamate (11c)

This compound was prepared from **10b** (0.175g, 0.7242mmol) and intermediate **2** (0.150g, 0.7242mmol) using described procedure B yielded 0.070g of off white solid (yield 22.4%). ^{1}H NMR (400 MHz, DMSO-d_6) δ 11.61 (s, 1H), 10.33 (s, 1H), 9.49 (d, *J* = 1.4 Hz, 1H), 9.20 (s, 1H), 9.13 (d, *J* = 1.4 Hz, 1H), 8.11 – 8.08 (m, 2H), 7.95 (dd, *J* = 8.0, 1.4 Hz, 1H), 7.68 – 7.63 (m, 1H), 7.59 – 7.54 (m, 2H), 7.32 – 7.24 (m, 2H), 7.19(td, *J* = 7.6, 1.6 Hz, 1H), 1.52 (s, 9H). $C_{23}H_{23}N_5O_4$ [M]: 433.46; MS (ESI) *m/z*: $[M+H]^+$: 434.20 $[M-H]^+$, 432.15

4.1.13. Preparation of *tert*-butyl (2-(5-benzamidopyrazine-2-carboxamido)-5-fluorophenyl) carbamate (11d)

Compound **10b** (0.175g, 0.7242 mmol) and compound **6** (0.164g, 0.7242 mmol) were mixed and reacted in presence of other reagents as described in procedure B which afforded 0.077g of pale pink powder(23.7%). ^{1}H NMR (400 MHz, DMSO-d_6) δ 11.61 (s, 1H), 10.31 (s, 1H), 9.51 (d, *J* = 1.4 Hz, 1H), 9.24 (s, 1H), 9.11 (d, *J* = 1.4 Hz, 1H), 8.11 – 8.08 (m, 2H), 7.79 (dd, *J* = 9.0, 6.1 Hz, 1H), 7.66 (t, *J* = 7.4 Hz, 1H), 7.56 (t, *J* = 7.6 Hz, 2H), 7.29 (dd, *J* = 10.4, 2.9 Hz, 1H), 7.09 (td, *J* = 8.5, 3.0 Hz, 1H), 1.51 (s, 9H). $C_{23}H_{22}FN_5O_4$ [M]: 451.45; MS (ESI) *m/z*: $[M+H]^+$: 452.20 $[M-H]^+$: 450.20

4.1.14. <u>Procedure C</u>: Preparation of 5-acetamido-N-(2-aminophenyl) pyrazine-2-carboxamide hydrochloride (12a)

Compound **11a** (0.1g, 0.3688mmol) was dissolved in 1 mL of DCM. The mixture was stirred in an ice bath for 15 minutes. 3 mL of 4M dioxane in HCl solution was added and stirred for 90 minutes. The reaction mixture was evaporated to dryness. The sticky mass was washed with n-pentane to get 0.060g of product **12a** in the form of pale yellow solid (yield 53%).^{1}H NMR (400 MHz, DMSO-d_6) δ 11.30 (s, 1H), 10.72 (s, 1H), 9.44 (d, *J* = 1.2 Hz, 1H), 9.04 (d, *J* = 1.3 Hz, 1H), 7.62 (d, *J* = 7.9 Hz, 2H), 7.55 (d, *J* = 7.7 Hz, 2H), 7.47 – 7.33 (m, 4H), 2.21 (s, 3H).^{13}C NMR (101 MHz, DMSO-d_6) δ 170.08, 162.24, 150.78, 142.55, 139.13, 133.68, 130.74, 127.96, 127.73, 127.27, 126.78, 126.27, 123.90. HPLC Rt: 4.663, this compound was deacetylated in HPLC column and deacetyalated form Rt was 3.070. LC-MS calculated for expected $C_{13}H_{13}N_5O_2$ [M]: 271.27; Found: [M-H]: 270

4.1.15. Preparation of 5-acetamido-N-(2-amino-4-fluorophenyl)pyrazine-2-carboxamide hydrochloride (12b)

Following procedure C, Compound **11b** (0.060g, 0.1542 mmol) was deprotected to get Compound **12b** as beige color powder (yield= 0.040g, 80%). ^{1}H NMR (400 MHz, DMSO-d_6) δ 11.25 (s, 1H), 10.27 (s, 1H), 9.42 (d, *J* = 1.2 Hz, 1H), 9.01 (d, *J* = 1.3 Hz, 1H), 7.43 (dd, *J* = 8.8, 6.0 Hz, 2H), 6.98 (dd, *J* = 10.2, 2.6 Hz, 1H), 6.84 (dd, *J* = 8.5, 2.5 Hz, 1H), 2.20 (s, 3H).^{13}C NMR (101 MHz, DMSO-d_6) δ 170.01, 161.97, 161.41, 159.01, 150.62, 142.36, 139.45, 133.63, 128.46, 128.36, 66.31, 23.80. HPLC Rt: 5.857, this compound was deacetylated in HPLC column and deacetyalated form Rt was 3.676. LC-MS calculated for expected $C_{13}H_{12}FN_5O_2$ [M]: 289.27; Found: $[M-H]^+$: 288

4.1.16. Preparation of N-(2-aminophenyl)-5-benzamidopyrazine-2-carboxamide hydrochloride (12c)

This compound was prepared from compound **11c** (0.070g, 0.1616mmol) following procedure C to get 0.055g of product in the form of off white solid (yield 93.2%).^{1}H NMR (400 MHz, DMSO-d_6) δ 11.62 (s, 1H), 10.71 (s, 1H), 9.58 (d, *J* = 1.4 Hz, 1H), 9.13 (d, *J* = 1.4 Hz, 1H), 8.13 – 8.08 (m, 2H), 7.69 – 7.54 (m, 5H), 7.47 (dd, *J* = 7.2, 2.0 Hz, 1H), 7.40 – 7.31 (m, 2H).^{13}C NMR (101 MHz, DMSO-d_6) δ 166.54, 162.14, 151.21, 142.42, 139.53, 134.93, 132.99, 132.63, 129.93, 128.49, 128.37, 127.10, 126.79, 126.58, 123.12. HPLC Rt: 5.555. LC-MS calculated for expected $C_{18}H_{15}N_5O_2$ [M]: 333.34; Found: $[M-H]^+$: 332

4.1.17. Preparation of N-(2-amino-4-fluorophenyl)-5-benzamidopyrazine-2-carboxamide hydrochloride (12d)

This compound was prepared from compound **11d** (0.065g, 0.1441mmol) following procedure C to get 0.050g of product in the form of beige color solid (yield 89.5%). ^{1}H NMR (400 MHz,

DMSO-d_6) δ 11.58 (s, 1H), 10.31 (s, 1H), 9.56 (d, *J* = 1.3 Hz, 1H), 9.10 (d, *J* = 1.3 Hz, 1H), 8.10 (d, *J* = 7.3 Hz, 2H), 7.69 – 7.39 (m, 5H), 7.10 (s, 2H), 6.94 (dd, *J* = 10.3, 2.5 Hz, 1H), 6.83 – 6.76 (m, 1H). ^{13}C NMR (101 MHz, DMSO-d_6) δ 166.48, 161.95, 161.52, 159.12, 151.03, 142.26, 139.83, 134.88, 133.00, 132.60, 128.48, 128.44, 128.35, 122.31, 66.32. HPLC Rt: 6.387 LC-MS calculated for expected $C_{18}H_{14}FN_5O_2$ [M]: 351.33; Found: $[M-H]^+$: 350

4.1.18. Preparation of methyl 6-aminopyrazine-2-carboxylate (14)

Methyl 6-(chloropyrazine)-2-carboxylate (**13**) (2 g, 0.0115mmol) was dissolved in 80 mL of DMSO. Sodium azide (3 g, 0.0463mmol) and triphenylphosphene (4.6 g, 0.1738mmol) were added and refluxed at 120°C for 4 hours. 20 mL of 1N HCl was added and the reaction was continued at 120°C for 2 hours. The mixture was cooled and neutralized by aqueous $NaHCO_3$ solution and product was extracted in ethyl acetate, dried with Na_2SO_4 which was then concentrated and dried with n-pentane to get 1.4 g of compound **14** as yellow solid (yield 82.4%).^{1}H NMR (400 MHz, DMSO-d_6) δ 8.28 – 8.27 (m, 1H), 8.07 (s, 1H), 6.90 (s, 2H), 3.84 (s, 3H). $C_6H_7N_3O_2$ [M]: 153.14; MS (ESI) *m/z*: $[M+H]^+$: 154.05

4.1.19. Preparation of methyl 6-acetamidopyrazine-2-carboxylate (15)

Compound **14** (1 g, 0.00653mmol) was heated at 90°C with an excess of acetic anhydride for 5 hours. The reaction mixture was evaporated and washed with $NaHCO_3$ solution. The product was extracted in ethyl acetate and concentrated organic layer was purified by column chromatography (EtOAc: Hexane; 4:6) to get 0.625g of intermediate **15** as white solid (yield 49.2%). ^{1}H NMR (400 MHz, DMSO-d_6) δ 11.25 (s, 1H), 9.53 (s, 1H), 8.90 (s, 1H), 3.92 (s, 3H), 2.15 (s, 3H). $C_8H_9N_3O_2$ [M]: 195.18; MS (ESI) *m/z*: $[M+H]^+$: 194.05

4.1.20. Preparation of 6-acetamidopyrazine-2-carboxylic acid (16)

Compound **15** (0.626g, 3.2102mmol) was dissolved in THF and stirred for 20 minutes at room temperature. Aqueous solution of lithium hydroxide (0.270g, 6.4205mmol) was added and stirred for 3 hours. The reaction mixture was neutralized by dilute aqueous solution of HCl and product was extracted in EtOAc. The organic layer was dried and concentrated to get sufficiently pure 0.330g of compound **16** as white solid (yield 56.8%).^{1}H NMR (400 MHz, DMSO-d_6) δ 11.19 (s, 1H), 9.50 (s, 1H), 8.88 (s, 1H), 2.16 (s, 3H). $C_7H_7N_3O_3$ [M]: 181.15; MS (ESI) *m/z*: $[M+H]^+$: 180.05

4.1.21. Preparation of tert-butyl (2-(6-acetamidopyrazine-2-carboxamido) phenyl) carbamate (17a)

This compound was synthesized by following procedure B from compound **16** (0.150g, 0.8287mmol) and compound **2** (0.190g, 0.9116mmol) which yielded 0.143 g of white solid compound **17a** (yield 46.5%). ^{1}H NMR (400 MHz, DMSO-d_6) δ 10.94 (s, 1H), 9.90 (s, 1H), 9.44 (s, 1H), 9.08 (s, 1H), 8.95 (s, 1H), 7.75 – 7.70 (m, 1H), 7.37 (dd, *J* = 6.4, 3.2 Hz, 1H), 7.25 – 7.20 (m, 2H), 2.19 (s, 3H), 1.43 (s, 9H). $C_{18}H_{21}N_5O_4$ [M]: 371.39; MS (ESI) *m/z*: $[M+H]^+$: 372.10 $[M-H]^+$: 370.15

4.1.22. Preparation of tert-butyl (2-(6-acetamidopyrazine-2-carboxamido)-5-fluorophenyl) carbamate (17b)

Compound **16** (0.160g, 0.8839mmol) and compound **6** (0.200g, 0.8839mmol) reacted according to procedure B and afforded 0.160g of product as off white solid (yield 46.5%). ^{1}H NMR (400 MHz, DMSO-d_6) δ 10.95 (s, 1H), 9.83 (s, 1H), 9.45 (s, 1H), 9.16 (s, 1H), 8.93 – 8.92 (m, 1H), 7.60 (dd, *J* = 8.9, 6.1 Hz, 1H), 7.39 (dd, *J* = 10.7, 2.9 Hz, 1H), 7.07 – 7.01 (m, 1H), 2.19 (s, 3H), 1.44 (s, 9H). $C_{18}H_{20}FN_5O_4$ [M]: 389.38; MS (ESI) *m/z*: $[M+H]^+$: 390.15 $[M-H]^+$: 388.20

4.1.23. Preparation of 6-acetamido-N-(2-aminophenyl) pyrazine-2-carboxamide hydrochloride (18a)

Compound **17a** (0.130g, 0.3504mmol) was deprotected following procedure C to get 0.105g of one final compound **18a** as white solid (yield 98.13%). ^{1}H NMR (400 MHz, DMSO-d_6) δ 10.98 (s, 1H), 10.57 (s, 1H), 9.49 (s, 1H), 8.98 (s, 1H), 7.69 (d, *J* = 7.3 Hz, 1H), 7.55 (d, J = 7.8 Hz, 1H), 7.42 (dd, *J* = 15.2, 7.0 Hz, 3H), 2.21 (s, 3H).^{13}C NMR (101 MHz, DMSO-d_6) δ 169.71, 162.21, 147.04, 142.25, 138.88, 137.76, 130.48, 127.94, 126.99, 126.89, 126.45, 124.02, 23.68. HPLC Rt: 4.663, this compound was deacetylated in HPLC column and deacetyalated form Rt was 3.070. LC-MS calculated for expected $C_{13}H_{13}N_5O_2$ [M]: 271.27; Found: $[M-H]^+$: 270

4.1.24. Preparation of 6-acetamido-N-(2-amino-4-fluorophenyl)pyrazine-2-carboxamide hydrochloride (18b)

This compound was prepared by following procedure C from compound **17b** (0.145g, 0.3727mmol) to get 0.120 g of another final compound **18b** as off white solid (yield 98.84%). ^{1}H NMR (400 MHz, DMSO-d_6) δ 11.03 (s, 1H), 10.01 (s, 1H), 9.48 (s, 1H), 8.94 (s, 1H), 7.89 (s, 3H), 7.53 (dd, *J* = 8.8, 6.0 Hz, 1H), 7.03 (dd, *J* = 10.1, 2.8 Hz, 1H), 6.88 (dd, *J* = 8.5, 2.7 Hz, 1H), 2.20 (s, 3H). ^{13}C NMR (101 MHz, DMSO-d_6) δ 169.76, 161.98, 161.33, 158.92, 147.04, 142.54, 138.74, 137.65, 127.72, 127.62, 106.44, 106.20, 23.68. HPLC Rt: 5.857, this compound was deacetylated in HPLC column and deacetyalated form Rt was 3.676. LC-MS calculated for expected $C_{13}H_{12}FN_5O_2$ [M]: 289.27; Found:$[M-H]^+$: 288.05

4.1.25. Preparation of methyl 5-phenylpyrazine-2-carboxylate (19)

This compound was prepared by following Suzuki coupling mechanism where methyl 5-(chloropyrazine)-2-carboxylate, a commercially available starting material **7** (2 g, 0.0115 mmol)

was reacted with phenyl boronic acid (1.4 g, 0.0115mmol) using bis(triphenylphosphine) palladium(II)dichloride (0.163g, 0.0002mmol) as catalyst, potassium carbonate (2.4g, 0.01737mmol) as base and 1,4-dioxane as solvent for 12 hour at 100°C. After completion of the reaction, the solvent was evaporated and crude was extracted in ethyl acetate and washed with water. The organic layer was dried over sodium sulfate and crude was purified by column chromatography (hexane: EtOAc; 9:1) to get 1 g of pure white crystalline solid intermediate **19** (yield 40.16%).^{1}H NMR (400 MHz, DMSO-d_6) δ 9.42 (d, *J* = 1.4 Hz, 1H), 9.25 (d, *J* = 1.4 Hz, 1H), 8.27 – 8.23 (m, 2H), 7.62 – 7.57 (m, 3H), 3.95 (s, 3H). $C_{12}H_{12}N_2O_2$ [M]: 214.22; MS (ESI) *m/z*: $[M+H]^+$: 215.10

4.1.26. Preparation of 5-phenylpyrazine-2-carboxylic acid (20)

Intermediate compound **20** (1g, 0.0046mmol) was reacted with lithium hydroxide (0.372g, 0.0093mmol) according to procedure A to get 0.9 g of white solid compound **20** (yield 96.7%). ^{1}H NMR (400 MHz, DMSO-d_6) δ 13.70 (s, 1H), 9.40 (d, *J* = 1.4 Hz, 1H), 9.24 (d, *J* = 1.4 Hz, 1H), 8.27 – 8.22 (m, 2H), 7.62 – 7.57 (m, 3H). $C_{11}H_8N_2O_2$ [M]: 200.19; MS (ESI) *m/z*: $[M+H]^+$: 201.05, $[M-H]^+$: 199.05

4.1.27. Preparation of tert-butyl (2-(5-phenylpyrazine-2-carboxamido) phenyl) carbamate (21a)

Compound **20** (0.2g, 1mmol) and compound **2** (0.208g, 1mmol) were reacted according to procedure B to get cream color solid (0.07g, 17.9%). ^{1}H NMR (400 MHz, DMSO-d_6) δ 10.24 (s, 1H), 9.44 (s, 1H), 9.25 (s, 1H), 8.16 – 8.11 (m, 2H), 7.81 (s, 1H), 7.54 (t, *J* = 12.7 Hz, 4H), 7.00 (t, *J* = 7.6 Hz, 1H), 6.85 – 6.74 (m, 2H), 1.40 (s, 9H). $C_{22}H_{22}N_4O_3$ [M]: 390.17; MS (ESI) *m/z*: $[M-H]^+$: 389.05

4.1.28. Preparation of tert-butyl (5-fluoro-2-(5-phenylpyrazine-2-carboxamido) phenyl) carbamate (21b)

Compound **20** (0.2g, 1mmol) and compound **6** (0.226g, 1mmol) were reacted according to procedure B to get compound **21b** as brown color solid (0.06g, yield 14.7%).^{1}H NMR (400 MHz, DMSO-d_6) δ 10.24 (s, 1H), 9.44 (s, 1H), 9.25 (s, 1H), 8.16 – 8.11 (m, 2H), 7.81 (s, 1H), 7.54 (t, *J* = 12.7 Hz, 4H), 6.85 – 6.74 (m, 2H), 1.40 (s, 9H). $C_{22}H_{21}FN_4O_3$ [M]: 408.43; MS (ESI) *m/z*: $[M-H]^+$: 407.05

4.1.29. Preparation of N-(2-aminophenyl)-5-phenylpyrazine-2-carboxamide hydrochloride (22a)

Compound **21a** (0.065g, 0.166mmol) was deprotected following procedure C to get final compound **22a** (0.054g, yield 99.1%) as pale pink solid. ^{1}H NMR (400 MHz, DMSO-d_6) δ 10.77 (s, 1H), 9.43 (d, *J* = 1.4 Hz, 1H), 9.35 (d, *J* = 1.4 Hz, 1H), 8.33 – 8.29 (m, 2H), 7.65 – 7.59 (m, 5H), 7.48 (dd, *J* = 6.9, 2.3 Hz, 1H), 7.40 – 7.33 (m, 2H). ^{13}C NMR (101 MHz, DMSO-d_6) δ 162.37, 153.85, 143.44, 142.75, 140.23, 135.01, 130.89, 129.78, 129.20, 127.37, 127.22, 126.94, 126.49, 123.06, 66.32. HPLC Rt: 6.823 LC-MS calculated for expected $C_{17}H_{14}N_4O$ [M]: 290.32; Found: $[M-H]^+$: 289

4.1.30. Preparation of N-(2-amino-4-fluorophenyl)-5-phenylpyrazine-2-carboxamide hydrochloride (22b)

Compound **21b** (0.055g, 0.134mmol) was deprotected following procedure C to get final compound **22b** (0.044g, yield 95.6%) as pale pink solid. ^{1}H NMR (400 MHz, DMSO-d_6) δ 10.77 (s, 1H), 9.43 (d, *J* = 1.4 Hz, 1H), 9.35 (d, *J* = 1.4 Hz, 1H), 8.33 – 8.29 (m, 2H), 7.65 – 7.59 (m, 5H), 7.40 – 7.33 (m, 2H).^{13}C NMR (101 MHz, DMSO-d_6) δ 162.74, 160.76, 158.36, 153.65,

142.08, 139.63, 133.54, 133.17, 128.82, 128.54, 128.45, 122.54, 119.09, 66.31. HPLC Rt: 7.144 LC-MS calculated for expected $C_{17}H_{13}FN_4O$ [M]: 308.31; Found: $[M-H]^+$: 307.05

4.1.31. <u>Procedure D:</u> Preparation of methyl 5-(phenylamino)pyrazine-2-carboxylate (23a)

Methyl 5-(chloropyrazine)-2-carboxylate (1.5 g, 0.00869 mmol), a commercially available starting material **7** was dissolved in 10 mL of 1,4-dioxane. Aniline (0.890g, 0.00956 mmol) and p-toluene sulphonic acid (2.25 g, 0.01303 mmol) were added and mixture was refluxed at 100°C for 12 hours. Reaction mixture was then concentrated and poured into water, extracted in EtOAc, dried over Na_2SO_4, filtered and evaporated. The crude was purified by column chromatography (EtOAc:Hexane; 3:7) to get 0.320 g of pale yellow solid compound **23a** (yield 16%). ^{1}H NMR (400 MHz, DMSO-d_6) δ 10.16 (s, 1H), 8.74 (s, 1H), 8.26 (s, 1H), 7.75 (d, *J* = 8.1 Hz, 2H), 7.37 (t, *J* = 7.7 Hz, 2H), 7.07 (t, *J* = 7.3 Hz, 1H), 3.84 (s, 3H). $C_{12}H_{11}N_3O_2$ [M]: 229.23; MS (ESI) *m/z*: $[M+H]^+$: 230.05, $[M-H]^+$: 228.05

4.1.32. Preparation of methyl 5-(benzylamino)pyrazine-2-carboxylate (23b)

Compound **23b** was also synthesized from methyl 5-(chloropyrazine)-2-carboxylate (1.5 g, 0.00869mmol) and benzylamine(1.39g,0.01303mmol) following procedure D to afford 0.7 g cream color solid compound (yield 33%). ^{1}H NMR (400 MHz, DMSO-d_6) δ 8.59 (d, *J* = 1.2 Hz, 1H), 8.48 (t, *J* = 5.8 Hz, 1H), 8.04 (d, *J* = 1.2 Hz, 1H), 7.34 (d, *J* = 4.4 Hz, 4H), 7.30 – 7.24 (m, 1H), 4.58 (d, *J* = 5.9 Hz, 2H), 3.79 (s, 3H). $C_{13}H_{13}N_3O_2$ [M]: 243.26; MS (ESI) *m/z*: $[M+H]^+$: 244.10, $[M-H]^+$: 242.05

4.1.33. Preparation of 5-(phenylamino) pyrazine-2-carboxylic acid (24a)

Methyl 5-(phenylamino)pyrazine-2-carboxylate (**23a**) (0.320g,1.3959mmol) was reacted with Lithium hydroxide (0.1 g, 4.1879mmol) following procedure A to get 0.3 g white solid

compound **24a** (yield 99.9%). ^{1}H NMR (400 MHz, DMSO-d_6) δ 12.91 (s, 1H), 10.09 (s, 1H), 8.72 (d, *J* = 1.1 Hz, 1H), 8.26 (d, *J* = 1.2 Hz, 1H), 7.77 – 7.74 (m, 2H), 7.39 – 7.33 (m, 2H), 7.06 (t, *J* = 7.4 Hz, 1H).). $C_{11}H_9N_3O_2$ [M]: 215.21; MS (ESI) *m/z*: $[M+H]^+$: 216.00, $[M-H]^+$: 214.05

4.1.34. Preparation of 5-(benzylamino) pyrazine-2-carboxylic acid (24b)

Compound **24b** was synthesized from compound **23a** (0.7g, 2.8775mmol) following procedure A. This reaction yielded 0.623g of product **24b** as white fluffy powder (yield 90%). ^{1}H NMR (400 MHz, DMSO-d_6) δ 12.61 (s, 1H), 8.58 (d, *J* = 1.2 Hz, 1H), 8.40 (t, *J* = 5.8 Hz, 1H), 8.03 (d, *J* = 1.3 Hz, 1H), 7.34 (d, *J* = 4.5 Hz, 4H), 7.26 (t, *J* = 4.5 Hz, 1H), 4.57 (d, *J* = 5.9 Hz, 2H). $C_{12}H_{11}N_3O_2$ [M]: 229.23; MS (ESI) *m/z*: $[M+H]^+$: 230.05, $[M-H]^+$: 228.05

4.1.35. Preparation of tert-butyl (2-(5-(phenylamino)pyrazine-2-carboxamido)phenyl) carbamate (25a)

Compound **24a** (0.140g, 0.6505mmol) was reacted with compound **2** (0.150g,0.7155mmol) according to procedure B to get 0.095g of white powder (yield 37%) ^{1}H NMR (400 MHz, DMSO-d_6) δ 10.11 (d, *J* = 8.4 Hz, 2H), 9.16 (s, 1H), 8.81 (s, 1H), 8.20 (s, 1H), 7.98 (d, *J* = 8.1 Hz, 1H), 7.78 (d, *J* = 8.2 Hz, 2H), 7.38 (t, *J* = 7.7 Hz, 2H), 7.25 (d, *J* = 6.0 Hz, 2H), 7.15 (t, *J* = 7.6 Hz, 1H), 7.06 (t, *J* = 7.3 Hz, 1H), 1.52 (s, 9H). $C_{22}H_{23}N_5O_3$ [M]: 405.45; MS (ESI) *m/z*: $[M+H]^+$: 406.20, $[M-H]^+$: 404.20

4.1.36. Preparation of tert-butyl (5-fluoro-2-(5-(phenylamino)pyrazine-2-carboxamido) phenyl) carbamate (25b)

Compound **25b** was synthesized from 5-(phenylamino) pyrazine-2-carboxylic acid (**24a**) (0.150g, 0.6976mmol) and *tert*-butyl (2-amino-5-fluorophenyl)carbamate (**6**) (0.197g, 0.7674mmol) following procedure B. The product obtained as pale pink powder 0.180g (yield 60.9%). ^{1}H NMR (400 MHz, DMSO-d_6) δ 10.09 (d, *J* = 17.9 Hz, 2H), 9.21 (s, 1H), 8.79 (d, *J* =

1.2 Hz, 1H), 8.21 (d, *J* = 1.2 Hz, 1H), 7.85 – 7.75 (m, 3H), 7.40 – 7.34 (m, 2H), 7.21 (dd, *J* = 10.2, 2.9 Hz, 1H), 7.11 – 7.03 (m, 2H), 1.51 (s, 9H). $C_{22}H_{22}FN_5O_3$ [M]: 423.44; MS (ESI) *m/z*: $[M+H]^+$: 424.15, $[M-H]^+$: 422.15

4.1.37. Preparation of tert-butyl (2-(5-(benzylamino)pyrazine-2-carboxamido) phenyl) carbamate (25c)

5-(benzylamino) pyrazine-2-carboxylic acid (**24b**) (0.250g, 1.0906mmol) and *tert*-butyl (2-aminophenyl) carbamate (**2**) (0.250g, 1.1996 mmol) were reacted following procedure B and afforded 0.220 g of pale cream powder compound **25c** (yield 48%). ^{1}H NMR (400 MHz, DMSO-d_6) δ 9.99 (s, 1H), 9.09 (s, 1H), 8.65 (s, 1H), 8.38 (t, *J* = 5.9 Hz, 1H), 7.98 – 7.95 (m, 2H), 7.36 (s, 2H), 7.35 (d, *J* = 2.0 Hz, 2H), 7.27 (t, *J* = 7.0 Hz, 1H), 7.22 (t, *J* = 6.8 Hz, 2H), 7.15 – 7.10 (m, 1H), 4.60 (d, *J* = 5.8 Hz, 2H), 1.48 (s, 9H). $C_{23}H_{25}N_5O_3$ [M]: 419.20; MS (ESI) *m/z*: $[M-H]^+$: 418.20

4.1.38. Preparation of tert-butyl (2-(5-(benzylamino)pyrazine-2-carboxamido)-5-fluorophenyl) carbamate (25d)

5-(benzylamino) pyrazine-2-carboxylic acid (**24b**) (0.195g, 0.8506 mmol) and *tert*-butyl (2-amino-5-fluorophenyl)carbamate (**6**) (0.240g, 0.9357 mmol) were reacted following procedure B. The product was obtained as pale pink powder; 0.200g (yield 53.7%). ^{1}H NMR (400 MHz, DMSO-d_6) δ 9.95 (s, 1H), 9.14 (s, 1H), 8.64 (s, 1H), 8.38 (s, 1H), 7.98 (s, 1H), 7.81 (t, *J* = 7.1 Hz, 1H), 7.35 (s, 4H), 7.27 (s, 1H), 7.19 (d, *J* = 10.2 Hz, 1H), 7.06 (t, *J* = 8.5 Hz, 1H), 4.60 (d, *J* = 4.9 Hz, 2H), 1.48 (s, 9H). $C_{23}H_{24}FN_5O_3$ [M]: 437.47; MS (ESI) *m/z*: $[M+H]^+$: 438.25, $[M-H]^+$: 436.20

4.1.39. Preparation of N-(2-aminophenyl)-5-(phenylamino)pyrazine-2-carboxamide hydrochloride (26a)

Compound **25a** (0.095g, 0.2345mmol) was deprotected following procedure C get one final compound **26a** as yellow color powder. (0.070 g, yield 87.3%).^{1}H NMR (400 MHz, DMSO-d_6) δ 10.56 (s, 1H), 10.52 (s, 1H), 8.82 (d, *J* = 1.2 Hz, 1H), 8.46 (d, *J* = 1.3 Hz, 1H), 7.84 (d, *J* = 7.7 Hz, 2H), 7.65 (d, *J* = 8.0 Hz, 1H), 7.58 (d, *J* = 7.9 Hz, 1H), 7.46 (t, *J* = 7.7 Hz, 1H), 7.40 – 7.38 (m, 1H), 7.38 – 7.34 (m, 2H), 7.06 (t, *J* = 7.4 Hz, 1H), 2.71 (d, *J* = 4.9 Hz, 1H). ^{13}C NMR (101 MHz, DMSO-d_6) δ 162.93, 153.73, 142.28, 139.60, 133.34, 133.25, 131.52, 128.82, 128.28, 127.12, 126.44, 126.33, 124.21, 122.60, 119.13. HPLC Rt: 6.285 LC-MS calculated for expected $C_{17}H_{15}N_5O$ [M]: 305.33; Found: $[M-H]^+$: 304

4.1.40. Preparation of N-(2-amino-4-fluorophenyl)-5-(phenylamino)pyrazine-2-carboxamide hydrochloride (26b)

tert-butyl (5-fluoro-2-(5-(phenylamino) pyrazine-2-carboxamido) phenyl) carbamate (**25b**) (0.130g, 0.3073mmol) was depretected as described in procedure C. Compound **26b** was obtained as orange color powder (0.1 g, yield 90.5%). ^{1}H NMR (400 MHz, DMSO-d_6) δ 10.47 (s, 1H), 10.24 (s, 1H), 8.79 (s, 1H), 8.42 (s, 1H), 7.82 (d, *J* = 8.5 Hz, 3H), 7.56 (dd, *J* = 8.9, 5.8 Hz, 1H), 7.40 – 7.34 (m, 3H), 7.22 (d, *J* = 9.6 Hz, 1H), 7.09 (d, *J* = 11.7 Hz, 1H), 7.04 (d, *J* = 8.4 Hz, 1H).^{13}C NMR (101 MHz, DMSO-d_6) δ 162.74, 160.76, 158.36, 153.65, 142.08, 139.63, 133.54, 133.17, 128.82, 128.54, 128.45, 122.54, 119.09, 66.31. HPLC Rt: 7.144 LC-MS calculated for expected $C_{17}H_{14}FN_5O$ [M]: 323.12; Found: $[M-H]^+$: 322

4.1.41. Preparation of N-(2-aminophenyl)-5-(benzylamino)pyrazine-2-carboxamide hydrochloride (26c)

The final compound **26c** was prepared by following procedure C from compound **25c** (0.120g, 0.2860mmol) to afford **26c** as yellow solid (0.103g, yield 100%). ^{1}H NMR (400 MHz, DMSO-d_6) δ 10.40 (s, 1H), 8.62 (d, *J* = 32.6 Hz, 2H), 8.13 (s, 1H), 7.63 (dd, *J* = 8.1, 1.3 Hz, 1H), 7.57 (dd, *J* = 7.9, 1.4 Hz, 1H), 7.47 – 7.41 (m, 1H), 7.39 – 7.32 (m, 6H), 7.27 (t, *J* = 7.4 Hz, 1H), 4.62 (s, 2H). ^{13}C NMR (101 MHz, DMSO-d_6) δ 163.19, 155.96, 142.99, 138.78, 131.66, 131.63, 128.39, 128.27, 127.38, 127.01, 126.98, 126.28, 126.17, 124.18, 66.31, 43.71. HPLC Rt: 5.355 LC-MS calculated for expected $C_{18}H_{17}N_5O$ [M]: 319.36; Found: $[M-H]^+$: 318

4.1.42. Preparation of N-(2-amino-4-fluorophenyl)-5-(benzylamino)pyrazine-2-carboxamide hydrochloride (26d)

Compound **26d,** another final compound was prepared from **25d** (0.1g, 0.2285mmol) following procedure C gave 0.85 g of brown solid (100% conversion). ^{1}H NMR (400 MHz, DMSO-d_6) δ 10.10 (s, 1H), 8.63 (d, *J* = 1.2 Hz, 1H), 8.11 (s, 1H), 7.53 (dd, *J* = 8.9, 5.9 Hz, 1H), 7.39 – 7.32 (m, 6H), 7.29 – 7.24 (m, 2H), 7.20 (dd, *J* = 9.6, 2.7 Hz, 1H), 7.05 (dd, *J* = 8.6, 2.6 Hz, 2H), 4.61 (s, 2H). ^{13}C NMR (101 MHz, DMSO-d_6) δ 162.98, 160.65, 158.27, 155.87, 142.70, 138.80, 131.82, 131.63, 128.38, 128.29, 127.38, 126.98, 126.17, 124.18, 66.32, 43.73 HPLC Rt: 6.082 LC-MS calculated for expected $C_{18}H_{26}FN_5O$ [M]: 337.35; Found: $[M-H]^+$: 336

4.2. HDAC inhibition assay

The enzyme inhibition assay was performed using HDAC colorimetric assay kit (BML-AK501, ENZO life sciences). Briefly, 5 µL of Hela nuclear extract (BML-KI137-0500), 10 µL of assay buffer (BML-KI143-0020), 10 µL of sample solution was added per well in a microtiter plate.

The reaction was started with addition of 25 µL Color de Lys® substrate solution (BML-KI138-0050). The reaction was incubated in for 30 minutes at 37°C which was terminated by addition of a 50 µl mixture of developer plus stop solution. The plate was incubated for 15 minutes at 37°C and absorbance was measured at 405 nm. All synthesized compounds along with **CI-994** and **BG-45** were screened at 5 µM concentration in duplicate. The promising three test compounds **26b**, **26c**, **26d** at concentration of 0.5 µM, 1 µM, 2 µM, 5 µM, 10 µM and 15 µM along with **BG-45** and **CI-994** (concentration range of 1 µM, 2 µM, 5 µM, 10 µM, 15 µM and 20 µM) were tested in duplicate to find out their IC_{50} values.

4.3. HDAC3/NCOR1 assay

This assay was performed using HDAC3/NCOR1 fluorometric drug discovery kit (BML-AK531, ENZO life sciences). Here, 10 µL of sample solution and 15 µL diluted HDAC3/NCOR1 complex solution (BML-KI574-0030) were added per well in microtiter plate and 25 µL Fluor de Lys® substrate solution (BML-KI177-0005) was added. The plate was incubated for 15 minutes at 37°C. To terminate the reaction, 50 µL of mixture of Fluor de Lys® developer II (BML-KI176-1250) and Trichostatin A ((BML-GR309-9090) was added per well and incubated for 45 minutes at 37°C. The fluorescence intensity was measured at Excitation wavelength 360 nm, Emission wavelength 460 nm using Spectramax M4 (Molecular Devices, USA). First all the synthesized compounds along with **CI-994** and **BG-45** were screened at 1µM concentration in duplicate. Compound **26b, 26c, 26d** and **BG-45** were evaluated at 0.05 µM, 0.1 µM, 0.25 µM, 0.5 µM, 1 µM and 2 µM for IC_{50} determination while **CI-994** was tested at 0.1 µM, 0.25 µM, 0.5 µM, 1 µM, 2 µM and 5 µM in duplicate.

4.4. Cell culture and drug treatment

The murine melanoma cell line (B16F10) and human cervical cancer cell line (HeLa) were procured from National center for cell science (NCCS, Pune, India) and cultured in Dulbecco's Modified Eagle Medium (DMEM) (Himedia Laboratories Pvt. Ltd., Mumbai, India), supplemented with 10% heat inactivated fetal bovine serum (Himedia Laboratories Pvt. Ltd., Mumbai, India) and 1 % of antibiotic solution (10000 U Penicillin and 10 mg Streptomycin per mL, Himedia Laboratories Pvt. Ltd., Mumbai, India). Cells were cultured at 37°C in humidified atmosphere with 5% CO_2. Stock solutions of all compounds were prepared in DMSO at a concentration of 100 mM and stored.

4.4.1. MTT assay

Antiproliferative activity of all the synthesized compounds was measured by in vitro MTT assay method. 5×10^3 cells were seeded in 96 well plate and incubated overnight. Cells were treated with **CI-994**, **BG-45** and test compounds in two doses 100µM and 10µM in triplicate and incubated for 72 hours. 50µl of 5mg/mL solution of MTT (3-(4,5-dimethylthiazol-2-yl)-2,5-diphenyltetrazolium bromide; Himedia Laboratories Pvt. Ltd., Mumbai, India) was added. After 4 hours of incubation, the formed formazan crystals were dissolved in DMSO and absorbance was measured at 570nm and 650nm using Spectramax M4 (Molecular Devices, USA).

For, IC_{50} measurement of four selected compounds (**12a, 22a, 26a, 26c, 26d**) along with **CI-994** and **BG-45**, the same procedure was followed as described above. The compounds were explored in a wide range of 0.781, 1.562, 3.125, 6.25, 12.5, 25, 50, 100 and 200 µM. The same experiment was repeated with another batch of cells.

4.4.2. Apoptosis assay

For apoptosis assay, $5x10^5$ B16F10 cells were seeded in 6 well plates and incubated overnight at 37°C. The following day, cells were treated with **CI-994**, **BG-45**, **26c** and **26d** and incubated for 72 hours. The cells were trypsinized and suspended in fresh media and centrifuged at 1000 rpm for 5 min at 4°C. The pellet was washed with ice cold PBS and centrifuged. The extent of apoptosis was measured by using Annexin V-FITC and PI dead cell apoptosis kit (Molecular probes, Thermo Fischer Scientific, USA).

4.4.3. Cell cycle analysis

Briefly, $5x10^5$ B16F10 cells were seeded in 6 well plates and incubated overnight at 37°C. The following day, cells were treated with **CI-994**, **BG-45**, **26c** and **26d** and incubated for 72 hours. Cells were trypsinized, centrifuged and washed twice with PBS and fixed with 70% ice cold ethanol and stored at -20°C for 24hours. The cells were centrifuged to remove ethanol, washed and resuspended in 500 µL PBS pH 7.4 containing RNAse (100 µg/mL) at room temperature for 20 min. Propidium iodide (PI) (50 µg/mL in PBS) was added to stain cellular DNA and kept in dark for 30 minutes. Flow cytometry analysis was performed and the percentage of cells in each phase of the cell cycle was estimated using the IDEAS Software (version 6.0).

5. Acknowledgement

This work was supported by SERB –DST (EMR/2016/001411) grant, Research Initiation Grant and Additional Competitive Research Grant from Birla Institute of Technology and Sciences-Pilani, Hyderabad to Balaram Ghosh. Prakruti Trivedi gratefully acknowledges Council of Scientific and Industrial Research (CSIR) for Senior Research Fellowship (SRF). Authors are thankful to the authority of BITS-Pilani, Hyderabad Campus, India and Jadavpur University, Kolkata, India for providing research facilities. Authors declare no conflict of interest.

6. References:

1. Fitzmaurice C, Dicker D, Pain A, Hamavid H, Moradi-Lakeh M, MacIntyre MF, et al. The global burden of cancer 2013. JAMA oncology. 2015;1(4):505-27.
2. Rosato RR, Grant S. Histone deacetylase inhibitors: insights into mechanisms of lethality. Expert opinion on therapeutic targets. 2005;9(4):809-24.
3. Xu W, Parmigiani R, Marks P. Histone deacetylase inhibitors: molecular mechanisms of action. Oncogene. 2007;26(37):5541.
4. Kouzarides T. Chromatin modifications and their function. Cell. 2007;128(4):693-705.
5. Mottamal M, Zheng S, Huang TL, Wang G. Histone deacetylase inhibitors in clinical studies as templates for new anticancer agents. Molecules. 2015;20(3):3898-941.
6. Frew AJ, Johnstone RW, Bolden JE. Enhancing the apoptotic and therapeutic effects of HDAC inhibitors. Cancer letters. 2009;280(2):125-33.
7. Amin SA, Adhikari N, Jha T. Structure–activity relationships of hydroxamate-based histone deacetylase-8 inhibitors: reality behind anticancer drug discovery. Future medicinal chemistry. 2017;9(18):2211-37.
8. Witt O, Deubzer HE, Milde T, Oehme I. HDAC family: What are the cancer relevant targets? Cancer letters. 2009;277(1):8-21.
9. Amin SA, Adhikari N, Jha T. Is dual inhibition of metalloenzymes HDAC-8 and MMP-2 a potential pharmacological target to combat hematological malignancies? Pharmacological research. 2017;122:8-19.
10. Gregoretti I, Lee Y-M, Goodson HV. Molecular evolution of the histone deacetylase family: functional implications of phylogenetic analysis. Journal of molecular biology. 2004;338(1):17-31.
11. Balasubramanian S, Verner E, Buggy JJ. Isoform-specific histone deacetylase inhibitors: the next step? Cancer letters. 2009;280(2):211-21.
12. Bertrand P. Inside HDAC with HDAC inhibitors. European journal of medicinal chemistry. 2010;45(6):2095-116.
13. Suresh P, Devaraj V, Srinivas NR, Mullangi R. Review of bioanalytical assays for the quantitation of various HDAC inhibitors such as vorinostat, belinostat, panobinostat, romidepsin and chidamine. Biomedical Chromatography. 2017;31(1).
14. Mann BS, Johnson JR, Cohen MH, Justice R, Pazdur R. FDA approval summary: vorinostat for treatment of advanced primary cutaneous T-cell lymphoma. The oncologist. 2007;12(10):1247-52.
15. Campas-Moya C. Romidepsin for the treatment of cutaneous T-cell lymphoma. Drugs of today (Barcelona, Spain: 1998). 2009;45(11):787-95.
16. Maiso P, Carvajal-Vergara X, Ocio EM, López-Pérez R, Mateo G, Gutiérrez N, et al. The histone deacetylase inhibitor LBH589 is a potent antimyeloma agent that overcomes drug resistance. Cancer research. 2006;66(11):5781-9.
17. Xie R, Yao Y, Tang P, Chen G, Liu X, Yun F, et al. Design, synthesis and biological evaluation of novel hydroxamates and 2-aminobenzamides as potent histone deacetylase inhibitors and antitumor agents. European journal of medicinal chemistry. 2017;134:1-12.
18. O'Connor OA, Horwitz S, Masszi T, Van Hoof A, Brown P, Doorduijn J, et al. Belinostat in patients with relapsed or refractory peripheral T-cell lymphoma: results of the pivotal phase II BELIEF (CLN-19) study. Journal of Clinical Oncology. 2015;33(23):2492.

19. Amin SA, Adhikari N, Jha T. Structure-activity relationships of HDAC8 inhibitors: Non-hydroxamates as anticancer agents. Pharmacological research. 2018.
20. Li X, Inks ES, Li X, Hou J, Chou CJ, Zhang J, et al. Discovery of the first N-hydroxycinnamamide-based histone deacetylase 1/3 dual inhibitors with potent oral antitumor activity. Journal of medicinal chemistry. 2014;57(8):3324-41.
21. Bhaskara S, Chyla BJ, Amann JM, Knutson SK, Cortez D, Sun Z-W, et al. Deletion of histone deacetylase 3 reveals critical roles in S phase progression and DNA damage control. Molecular cell. 2008;30(1):61-72.
22. Bhaskara S, Knutson SK, Jiang G, Chandrasekharan MB, Wilson AJ, Zheng S, et al. Hdac3 is essential for the maintenance of chromatin structure and genome stability. Cancer cell. 2010;18(5):436-47.
23. Bose P, Dai Y, Grant S. Histone deacetylase inhibitor (HDACI) mechanisms of action: emerging insights. Pharmacology & therapeutics. 2014;143(3):323-36.
24. Huang Y-S, Chang C-C, Lee S-S, Jou Y-S, Shih H-M. Xist reduction in breast cancer upregulates AKT phosphorylation via HDAC3-mediated repression of PHLPP1 expression. Oncotarget. 2016;7(28):43256.
25. Hanigan TW, Aboukhatwa SM, Taha TY, Frasor J, Petukhov PA. Divergent JNK Phosphorylation of HDAC3 in Triple-Negative Breast Cancer Cells Determines HDAC Inhibitor Binding and Selectivity. Cell chemical biology. 2017;24(11):1356-67. e8.
26. Chen C-q, Chen C-s, Chen J-j, Zhou L-p, Xu H-l, Jin W-w, et al. Histone deacetylases inhibitor trichostatin A increases the expression of Dleu2/miR-15a/16-1 via HDAC3 in non-small cell lung cancer. Molecular and cellular biochemistry. 2013;383(1-2):137-48.
27. Liu C, Liu L, Shan J, Shen J, Xu Y, Zhang Q, et al. Histone deacetylase 3 participates in self-renewal of liver cancer stem cells through histone modification. Cancer letters. 2013;339(1):60-9.
28. Wilson AJ, Byun D-S, Popova N, Murray LB, L'Italien K, Sowa Y, et al. Histone deacetylase 3 (HDAC3) and other class I HDACs regulate colon cell maturation and p21 expression and are deregulated in human colon cancer. Journal of Biological Chemistry. 2006;281(19):13548-58.
29. Zhang L, Hong Z, Zhang R-r, Sun X-z, Yuan Y-f, Hu J, et al. Bakkenolide A inhibits leukemia by regulation of HDAC3 and PI3K/Akt-related signaling pathways. Biomedicine & Pharmacotherapy. 2016;83:958-66.
30. Harada T, Ohguchi H, Grondin Y, Kikuchi S, Sagawa M, Tai Y-T, et al. HDAC3 regulates DNMT1 expression in multiple myeloma: therapeutic implications. Leukemia. 2017;31(12):2670.
31. Jiang Y, Ortega-Molina A, Geng H, Ying H-Y, Hatzi K, Parsa S, et al. CREBBP inactivation promotes the development of HDAC3-dependent lymphomas. Cancer discovery. 2017;7(1):38-53.
32. Shan X, Fu Y-S, Aziz F, Wang X-Q, Yan Q, Liu J-W. Ginsenoside Rg3 inhibits melanoma cell proliferation through down-regulation of histone deacetylase 3 (HDAC3) and increase of p53 acetylation. PloS one. 2014;9(12):e115401.
33. Libý P, Kostrouchová M, Pohludka M, Yilma P, Hrabal P, Sikora J, et al. Elevated and deregulated expression of HDAC3 in human astrocytic glial tumours. Folia biologica. 2006;52(1/2):21.
34. Gupta P, C Reid R, Iyer A, J Sweet M, P Fairlie D. Towards isozyme-selective HDAC inhibitors for interrogating disease. Current topics in medicinal chemistry. 2012;12(14):1479-99.

35. Loprevite M, Tiseo M, Grossi F, Scolaro T, Semino C, Pandolfi A, et al. In vitro study of CI-994, a histone deacetylase inhibitor, in non-small cell lung cancer cell lines. Oncology Research Featuring Preclinical and Clinical Cancer Therapeutics. 2005;15(1):39-48.
36. Ryan QC, Headlee D, Acharya M, Sparreboom A, Trepel JB, Ye J, et al. Phase I and pharmacokinetic study of MS-275, a histone deacetylase inhibitor, in patients with advanced and refractory solid tumors or lymphoma. Journal of Clinical Oncology. 2005;23(17):3912-22.
37. Salisbury CM, Cravatt BF. Activity-based probes for proteomic profiling of histone deacetylase complexes. Proceedings of the National Academy of Sciences. 2007;104(4):1171-6.
38. Falkenberg KJ, Johnstone RW. Histone deacetylases and their inhibitors in cancer, neurological diseases and immune disorders. Nature reviews Drug discovery. 2014;13(9):673.
39. Marson CM, Matthews CJ, Yiannaki E, Atkinson SJ, Soden PE, Shukla L, et al. Discovery of potent, isoform-selective inhibitors of histone deacetylase containing chiral heterocyclic capping groups and a N-(2-aminophenyl) benzamide binding unit. Journal of medicinal chemistry. 2013;56(15):6156-74.
40. Marson CM, Matthews CJ, Atkinson SJ, Lamadema N, Thomas NSB. Potent and selective inhibitors of histone deacetylase-3 containing chiral oxazoline capping groups and a N-(2-aminophenyl)-benzamide binding unit. Journal of medicinal chemistry. 2015;58(17):6803-18.
41. Hsieh H-Y, Chuang H-C, Shen F-H, Detroja K, Hsin L-W, Chen C-S. Targeting breast cancer stem cells by novel HDAC3-selective inhibitors. European journal of medicinal chemistry. 2017;140:42-51.
42. Amin SA, Adhikari N, Jha T, Ghosh B. Designing potential HDAC3 inhibitors to improve memory and learning. Journal of Biomolecular Structure and Dynamics. 2018; In press. DOI: 10.1080/07391102.2018.1477625
43. Minami J, Suzuki R, Mazitschek R, Gorgun G, Ghosh B, Cirstea D, et al. Histone deacetylase 3 (HDAC3) as a novel therapeutic target in multiple myeloma. Leukemia. 2014;28(3):680.
44. Reis SA, Ghosh B, Hendricks JA, Szantai-Kis DM, Törk L, Ross KN, et al. Light-controlled modulation of gene expression by chemical optoepigenetic probes. Nature chemical biology. 2016;12(5):317.
45 Kandalkar SR, Kaduskar RD, Ramaiah PA, Barawkar DA, Bhuniya D, Deshpande AM. Highly efficient one-pot amination of carboxylate-substituted nitrogen-containing heteroaryl chlorides via Staudinger reaction. Tetrahedron Letters. 2013;54(5):414-8.
46 Staudinger H, Meyer J. Über neue organische phosphorverbindungen III. Phosphinmethylenderivate und phosphinimine. Helvetica Chimica Acta. 1919;2(1):635-46.
47. Serebryannyy LA, Cruz CM, De Lanerolle P. A role for nuclear actin in HDAC 1 and 2 regulation. Scientific reports. 2016;6:28460.
48. Manal M, Chandrasekar M, Priya JG, Nanjan M. Inhibitors of histone deacetylase as antitumor agents: a critical review. Bioorganic chemistry. 2016;67:18-42.

Graphical abstract